Virtual Reality (2025) 29:28
https://doi.org/10.1007/s10055-024-01078-w

ORIGINAL ARTICLE

Creating adapted environments: enhancing accessibility in virtual reality for upper limb rehabilitation through automated element adjustment

V. Herrera[1] · J. Albusac[1] · J. J. Castro-Schez[1] · C. González-Morcillo[1] · D. N. Monekosso[2] · S. Pacheco[3] · R. Perales[4] · A. de los Reyes-Guzmán[3]

Received: 26 July 2024 / Accepted: 27 November 2024

Abstract

In the last decade, Virtual Reality (VR) has emerged as a promising tool for upper limb rehabilitation, effectively complementing conventional therapies. However, one of the main challenges lies in designing virtual environments that adapt to the specific needs of each patient, considering their unique motor limitations. An inadequately adapted environment can result in overexertion and the inability to perform exercises, negatively affecting both the patient's motivation and their recovery. This article hypothesizes that automatic calibration and dynamic object adjustment algorithms in virtual reality environments improve accessibility and efficiency in upper limb rehabilitation exercises for patients with SCI. For this purpose, we present an innovative calibration method that individually identifies and maps motor limitations on the left and right sides of the body. As a result, an irregular volume, formed by the interconnection of three elliptical shapes, is generated that envelops the patient and represents their safe range of movements. Furthermore, a second method is introduced that automatically readjusts the location of objects within the virtual environment to the safe space generated, optimizing the patient's accessibility and interaction with therapy elements. To test the results, an immersive VR environment was designed in which the aforementioned methods were applied for the automatic placement of virtual elements in the peripersonal space (PPS) of the participants. Testing has been carried out at the Hospital Nacional de Parapléjicos in Toledo (HNPT) with patients suffering from spinal cord injuries (SCI) and healthy participants who are SCI specialists. The quantitative results obtained demonstrate that this dynamic adjustment of the environment allows for adaptation that leads to a 100% success rate in task completion after the automatic adjustment, compared to a 62.5% success rate when using a configuration with virtual elements adapted to the motor capabilities of a healthy person (for both healthy participants and patients). This adjustment not only facilitates a greater number of exercise repetitions, but also reduces the time needed to access each object, with an average reduction in time of 47.94% across the entire sample. This reduction is even more significant when considering only the group of SCI patients, with a reduction of 53.78%. Additionally, the qualitative evaluation complements the study with a perception of ease of use for the calibration (mean = 1.29 ± 0.46) and low complexity in accessing the interactive objects after the automatic adjustment (mean = 1.12 ± 0.45). These results demonstrate the effectiveness of the proposed algorithms and the improved user experience.

Keywords Serious games · Virtual reality · Adaptation · Accessibility · Upper-limb rehabilitation · Spinal cord injury

✉ V. Herrera
vanesa.herrera@uclm.es

[1] Department of Information Technologies and Systems, University of Castilla-La Mancha, Paseo de la Universidad 4, 13071 Ciudad Real, Spain

[2] Department of Computer Science, Durham University, Stockton Road, Durham DH1 3LE, UK

[3] Biomechanics and Technical Aids Unit, National Hospital for Paraplegics, Carretera de la Peraleda s/n, 45004 Toledo, Spain

[4] Occupational Therapy Unit, National Hospital for Paraplegics, Carretera de la Peraleda s/n, 45004 Toledo, Spain

1 Introduction

Virtual reality (VR), although not an emerging technology, has experienced remarkable growth over the past five years. This trend has been reflected in the commitment of technology giants such as Microsoft, Apple, Meta or HTC, who have invested in developing their own VR devices and bringing them to market at more affordable prices. Technological improvements, cost reductions and a wide range of applications and games have led to widespread use.

In addition, evolving APIs have simplified the development of virtual environments, offering advanced functionalities such as hand tracking, interaction with virtual objects and a more realistic physics engine. These developments have catalysed an increase in the number of projects and research in various fields. This growth is attributed to more affordable devices and a broad spectrum of applications, including entertainment (Valente et al. 2016; Cheng and Wang 2022; Ying et al. 2022), art (Lin et al. 2020; Kim and Lee 2022; Chrysanthakopoulou et al. 2022), medicine and healthcare (Javaid and Haleem 2020; Venkatesan et al. 2021; Fujihara and Ukimura 2022) and education (Paíno Ambrosio et al. 2020; Wang et al. 2022; Soliman et al. 2021; Hutson and Fulcher 2023), among others.

As the use of VR becomes more widespread, its potential to reach a wider and more diverse audience becomes evident. This growing diversity of VR user profiles reinforces the importance of designing virtual environments that are accessible, inclusive, personalized and adaptable (Kalouaz and Rooney 2021; Lagos Rodriguez et al. 2022; Dudley et al. 2023) to individual needs and capabilities, especially for people with motor or cognitive limitations (Hoppe et al. 2020; Lagos Rodriguez et al. 2022). Emphasizing inclusive design principles in VR development is not only crucial to broaden the user base, but also to enhance their experience, making VR a more inclusive and equitable technology.

A notable advancement facilitating this accessibility and adaptation in VR is the introduction of direct hand-tracking technology in head-mounted display (HMD) devices. This innovation allows users to interact with the virtual world using their own hands, without the need for controllers or joysticks, making the interaction more intuitive, natural, and simple (Buckingham 2021). Such advancements in HMD devices illustrate the first form of adaptation within VR environments, catering specifically to users who previously could not engage with VR due to reduced mobility or diminished manipulation capabilities in their hands (Juan et al. 2022).

Despite significant advances, there are still important limitations in adapting these technologies for people with reduced manual dexterity. *Manual dexterity* is an umbrella term for a variety of hand skills and performances, including reaction time, hand preference, wrist flexion speed, finger touch speed, pointing accuracy, hand stability, and arm stability (McGrath 2015). This capacity is necessary for everyday tasks and can be severely impacted in certain populations. Numerous groups face challenges in manual dexterity due to specific conditions. For instance, the elderly often see their manual capabilities decline due to aging, affecting their grip strength and complicating daily activities (Martin et al. 2015). Stroke survivors and individuals with conditions like cerebral palsy or spinal cord injury (SCI) also experience significant manual impairments (Brown 2006; Lee et al. 2022; Golubović and Slavković 2014).

Specifically, in the field of rehabilitation, adapting VR environments to accommodate user motor limitations is particularly relevant. Essentially, upper limb motor recovery rehabilitation involves repeating exercises where patients typically manipulate one or several objects to perform actions involving movement (Martin and Silvestri 2013). For patients with upper limb injuries and reduced mobility, creating and adapting an accessible virtual environment requires specific adaptations related to the type and mechanisms of interaction. This means that the environment should not only be user-friendly and customisable, focusing on the rehabilitation exercises to be performed, but also capable of recognizing various types of interactions such as ray casting (Pietroszek 2018), object pushing (Kang et al. 2020), or grasping (Blaga et al. 2024), taking into account the specific conditions of the fingers and hands.

With regard to the latter, grasping mechanics in virtual environments present additional complexity because they need to accommodate a wide range of user needs and abilities. Specifically: (a) It must recognize different types of functional grasps and not be limited to those widely recognized and utilized by VR applications, such as the grip used for selecting objects which involves a full pinch (nearly touching the fingers together) (Meta 2024; Using Apple Vision Pro for Advanced Interaction 2023). It also requires adapting to the object's volume. (b) For patients unable to perform these grasps, such as those with significant impairments, an automatic grasping feature enables them to interact with objects by automating the grasp when their hand approaches the object. (c) Regardless of the type of grasp, it is necessary that all objects are positioned within the patient's peripersonal space (PPS), tailored to each individual's Range of Motion (ROM).

Failure to address these adaptation needs of VR rehabilitation environments can have negative consequences. If different types of grasps, including automatic grasps, are not recognised, or if they are not adapted to the volume of the object, patients may not be able to use virtual environments for rehabilitation as they cannot interact properly. On the other hand, this lack of grip adaptation can lead to frustration when they are unable to complete tasks, which can have a negative impact on the overall rehabilitation process with poorly executed tasks or an increased risk of abandonment. Finally, if virtual elements are placed outside the patient's ROM, this may not only cause frustration and introduce biases in the use of VR environments, but may also lead to overexertion and unwanted compensatory movements, which may compromise the patient's safety and effectiveness.

In this article, we address the adaptation of virtual environments for upper limb rehabilitation, focusing on the three-dimensional arrangement of virtual elements that require direct manipulation by the patient. A global approach specially designed for patients with SCI is proposed. The proposal includes an automatic calibration process, focusing on the physical characteristics of the patient and considering the possible asymmetry in the motor capabilities of the right and left upper limbs. After obtaining the physical boundaries within the patient's PPS, these are contemplated in any other virtual scenario, where the output data from the calibration serves as input data for two algorithms: one to detect elements outside the calibrated area and another to relocate elements within the safe boundaries. In essence, the aim is to ensure that exercises performed in a seated and static position (such as a wheelchair), which require the direct manipulation of objects within the PPS, are accessible to the patient, adapted to their ROM and flexible according to the characteristics of the exercise.

The main hypothesis of this study is that dynamic adaptation of virtual objects within a personalized three-dimensional space, calibrated to each patient's specific ROM, can improve accessibility in upper limb rehabilitation. Specifically for SCI patients, the detection and repositioning of elements within the virtual environment is expected to optimize the effectiveness of rehabilitation exercises, potentially improving task performance and providing a safer environment.

To evaluate the positioning adaptation of virtual elements post-calibration, a tailored virtual environment was developed, featuring five blocks strategically placed within the virtual space. Participants are tasked to relocate these blocks from their starting positions to a designated central target through three different test environments: the first with elements out of reach to assess spatial awareness (no calibration - scenario not adapted), the second adjusted to the mobility range of an average healthy individual, and the third tailored to each patient's pre-calibrated personal space.

Using the calibration data, three ellipses are generated in the *XZ*, *XY* and *YZ* planes that form an elliptical volume for the right side, another one for the left side, and a zone that determines the central area of the patient. Both the elliptical volumes and the central area depend on the patient's degree of mobility and are obtained independently for each of the two lateralities. In addition, the environment created to test the suitability of the calibrated area and when applying the detection and automatic adjustment algorithms has been designed using interaction with an automatic grasping mechanism. This configuration ensures that the results obtained are free of biases associated with the manipulative ability of the participant, allowing for a more accurate and equitable assessment of the effectiveness of the adapted rehabilitation environment.

The evaluation of our proposal is conducted through both quantitative and qualitative methods. During experimentation, kinematic data is collected, which, along with other parameters, facilitates a quantitative assessment of exercise performance. This data is used to verify that the movements executed by the patient are within the limits established as safe and adapted to their motor capacity. Alongside this data, the number of blocks moved correctly and the time required to complete the tasks are recorded, comparing results between an environment initially adapted for a healthy patient and one personalized for the patient being evaluated. The qualitative evaluation is carried out using a questionnaire designed to be concise and not overburden the patient. The key questions focus on their perception of the complexity of the calibration process, the adequacy of the environment to their motor capabilities, and the correct placement of elements after the application of the automatic detection and adjustment algorithms.

The rest of the article is structured as follows. Related work is presented in Sect. 2, presenting work and studies related to the accessibility, inclusion and personalization of VR environments, as well as their use for upper limb rehabilitation. Section 3 deals with the background of the study presented, explaining why the need for adapting immersive environments according to the patient's ROM for upper limb rehabilitation arises, as well as the project behind it. Section 4 describes in detail the asymmetric calibration algorithms, as well as the automatic detection and adjustment algorithms in order to relocate virtual objects within the user's PPS, adapting them to their ROM. Section 5 is devoted to the test environment, including a description of the immersive virtual environment designed to perform the test, its configuration, the metrics used to evaluate the algorithms and the analysis of the quantitative and qualitative results obtained. Finally, Sect. 6 contains the conclusions of this research and the description of future work.

2 Related work

The placement of objects within the virtual environment is determined by taking into account the physical limitations of the player, including bodily characteristics and the boundaries of the physical space being tracked, which is essential to provide a safe and effective VR experience (Vlahovic et al. 2022).

The growing use of immersive VR in a variety of environments points to a landscape in which the adaptation of applications and interaction mechanisms is a major focus. As VR technologies become more accessible, more and more studies are exploring the creation of VR spaces adapted to people with different abilities.

A notable development in this area is the concept of *Inclusive Immersion* introduced by Dudley et al. (2023). This research emphasises making design decisions that maximise usability for the widest possible population, based on an understanding of the diversity of users. This approach emphasises the moral imperative to make technological advances accessible to all, the recognition of the proven value of VR and AR as assistive and rehabilitative technologies, the commercial benefits of reaching the widest possible user base, and the notion that good design often leads to better usability for all.

Building on the foundation of Inclusive Immersion, Othman et al. (2024) present a comprehensive framework aimed at ensuring that the metaverse is accessible to all, with particular emphasis on the need for environments that are tailored to the unique needs of each user. Mott et al. (2019) further contribute to the discourse on accessibility in VR, identifying critical areas that encompass content and interaction techniques to device and hardware accessibility. Additionally, another framework by Vlahovic et al. (2022) explores various aspects of VR gaming mechanics with a significant focus on the adaptability of the VR environment. One of the critical aspects is the placement of objects within the virtual space, which is carefully determined by considering the physical limitations and bodily characteristics of the player, as well as the boundaries of the physical space being tracked.

The importance of personalized VR environments is reflected in the work of Lagos Rodriguez et al. (2022), who demonstrates the value of VR in rehabilitation by allowing patients to interact with natural movements, such as their own hands, simulating everyday activities to train various physical and cognitive skills. Extending these principles, the INTERACT framework by Vlahovic et al. (2022) provides a methodological basis for the evaluation of the game mechanics of VR games. This framework includes a taxonomy of interaction mechanisms that captures the importance of symmetry, synchrony and orientation accuracy required in VR games. Mechanisms that must adapt to the constraints imposed by the user's bodily characteristics and the limits of the physical space being tracked. It also advocates the automation of the adjustment process within VR environments based on user-specific calibrations.

Continuing with the importance of a patient-centered approach and intuitive interaction, the results of the work by Postolache et al. (2021) suggest that interaction with the user's hands together with HMD could improve motivation. This approach be well accepted by motor rehabilitation patients and help to complete exercise therapy at home. Soomal et al. (2020) showcases the application of VR in enhancing rehabilitation for Multiple Sclerosis (MS) patients through engaging games, demonstrating VR's potential in providing adaptable and enjoyable home-based therapy.

In terms of studies related to the accessibility of interaction techniques in VR environments, Franz et al. (2023) show how accessibility, along with other factors such as workload and user experience, influences the selection of locomotion techniques by people with upper limb motor disabilities, showing the importance of offering customisable options that are adapted to individual preferences.

In the current literature on upper limb rehabilitation using VR, we found several approaches using immersive VR with controllers. Lim et al. (2020) used HTC VIVE VR RehabWare, demonstrating functional improvements, especially in grip strength and K-SCIM score. Phelan et al. (2021) showed significant improvements in functional abilities in children with motor disabilities. In this study it is mentioned that the weight of the controllers could cause discomfort. In addition to the need to adapt the VR scenarios to the patient's range of motion.

The pilot study by Tokgöz et al. (2023) on the integration of VR in rehabilitation was generally well received. However, important concerns were expressed about the safety of using immersive VR, especially in an unsupervised manner, such as the risk of falls and injuries due to the immersive nature of VR.

Without the use of controllers, Xiao et al. (2022) employed the Kinect sensor to detect compensatory movements, avoiding additional controllers and improving the accuracy of rehabilitative exercises.

Finally, Mc Kittrick et al. (2023) explored immersive rehabilitation using controller-free VR games. This study underlines the importance of fun and engagement in VR tasks. It also suggests the need for adjustable tolerance levels to suit the patient's abilities. In this study one of the participants indicated difficulty in releasing objects in the virtual environment which the problem of some patients not only in grasping virtual objects but also in releasing them.

In addition to studies on the adaptation of VR environments, it is also crucial to discuss the importance of ROM in contexts such as rehabilitation. The rehabilitation process starts with the accurate identification of limitations in ROM in order to formulate effective strategies aimed at its recovery. Recent advances in mechatronic systems based on inertial sensors present a promising method for the accurate assessment of ROM in clinical and home environments, enabling efficient three-dimensional measurements that facilitate detailed assessment and monitoring of motor recovery. In this context, the study presented by RajKumar et al. (2020) introduces a mechatronic approach for designing and developing a Wearable Inertial Sensor system for the triplanar assessment of the upper extremity's ROM, showcasing the potential for detailed monitoring and assessment in clinical and home settings.

Other studies, such as the one introduced by Wazir et al. (2022), investigate the measurement of ROM without the employment of wearable devices. Instead, Digital Voice Assist Devices are utilized to conduct ROM assessments through 2D pose estimation techniques to infer the 3D pose of limbs. This research underscores the criticality of an initial calibration stage that tailors the system to the physical dimensions and motion capabilities of the user, thereby enhancing the precision and effectiveness of ROM evaluations.

While there are a number of serious VR-based platforms and games for rehabilitation, recent studies still remarks significant areas for improvement. Our proposal focuses on the advantages of immersive virtual environments, taking advantage of the patient's hands to perform the exercises and adapting the interaction mechanisms to the patient's ROM, especially in the PPS. Our research focuses not only on improving accessibility and adaptation to the patient's motor skills, but also on maximising the benefits offered by these environments, always ensuring that the interaction takes place in a safe environment. This is achieved by taking into account the asymmetric mobility characteristics, calibration settings focused on common exercise characteristics (static and seated position), and capturing the necessary data from the calibrated area to be used in a highly configurable way depending on the exercise and the patient.

3 Background

After analysing related work on existing technology for upper limb rehabilitation based on VR, we identified a clear need to adapt and make VR environments accessible to the specific needs of each patient. In response to these needs, *Rehab-Immersive* (Herrera et al. 2023) was created, a project in collaboration with the Hospital Nacional de Parapléjicos de Toledo (HNPT) in which the present work is framed. Rehab-Immersive is a platform specifically designed to complement traditional therapy for people with SCI during rehabilitation. The platform integrates a series of serious games specifically designed and adapted for people with SCI and centered on their needs (see Fig. 1).

Specifically, the platform presents a multilayer architecture. From top to bottom, the upper layer hosts a series of serious games aimed at upper limb rehabilitation (see Fig. 2). Common functionalities across these games are encapsulated in a core responsible for body tracking functionalities and hand-based interaction mechanisms. Additionally, the platform includes AI modules that adapt the environment to each patient's specific conditions. The platform also has the capability to record spatiotemporal data generated by each patient during exercise sessions. In the lower layers, patients can use the serious games via a VR headset, while healthcare professionals can access and objectively analyze session data to assess patient progress. This team of professionals, composed of biomechanical engineers and occupational therapists from HNPT, also plays a significant role in the design of the overall architecture and the experimentation. They are responsible for designing the mechanics of the serious games, providing their perspective in functional validation, and ensuring that the system guarantees patient safety at all times.

One of the major difficulties in the design of these serious games is that they must be adapted to the particular needs of each patient. In cervical SCI, upper limb functionality and mobility vary significantly depending on the injury level. C4 injuries result in minimal muscle functionality, while lower levels such as C5 and C6 allow some shoulder mobility and elbow flexion, and wrist extension facilitates tenodesis grip. At C7 and C8 levels, patients experience improved shoulder and arm control, enabling more complex movements and precise object manipulation thanks to the ability to flex and extend the fingers (Mateo et al. 2015).

For these reasons, the platform integrates a set of serious games designed with a patient-centered approach. All games share a common core that unifies and facilitates the creation of new developments. Within the core, they incorporate various interaction mechanisms such as grasping, pushing and throwing beams, adapted to exercise requirements and individual patient characteristics.

In addressing accessibility and adaptation of VR environments from various angles, the platform emphasises the understanding of different types of grasping. This includes the development of an automatic grasping mechanism for patients who lack functional grasping ability, as well as the adaptation of the degree of grasping depending on the volume of the virtual object. As introduced at the beginning of the article, it is crucial that patients with SCI have

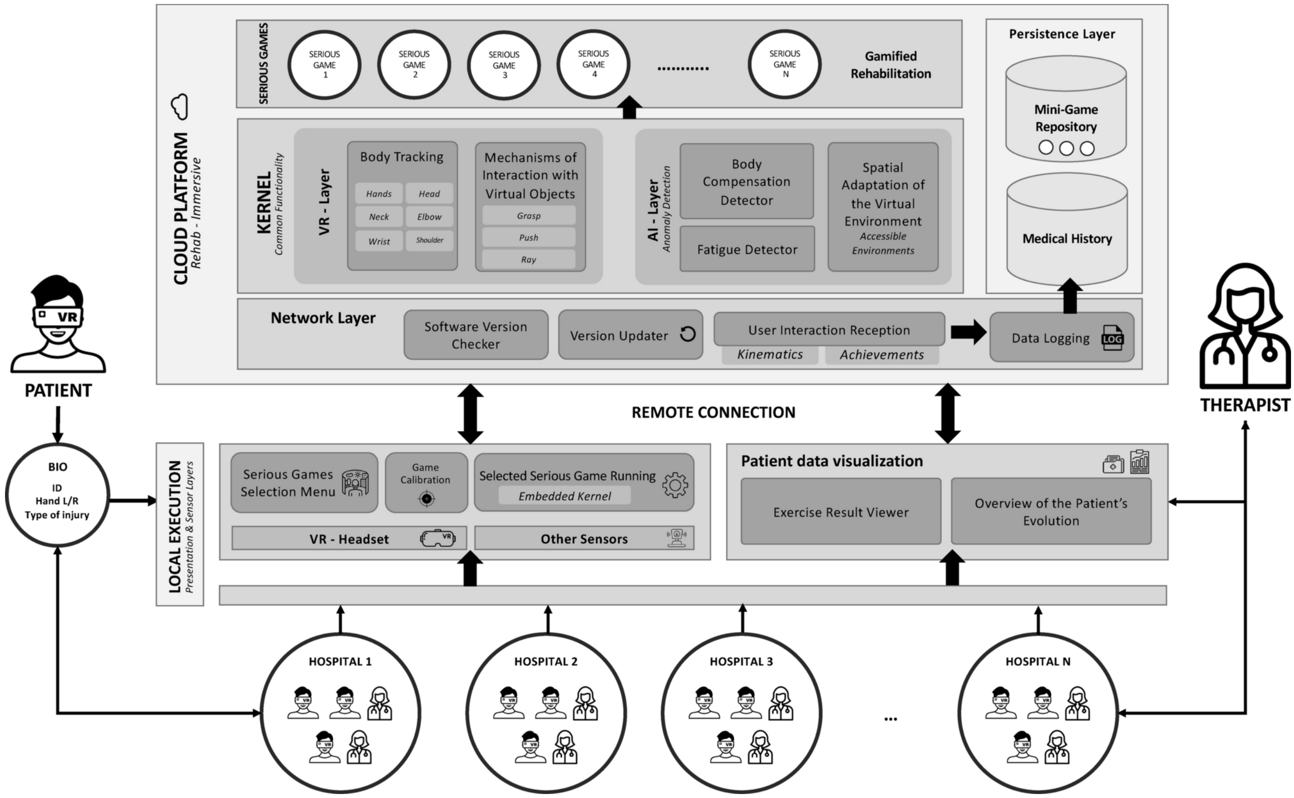

Fig. 1 Global overview of the rehab-immersive platform architecture

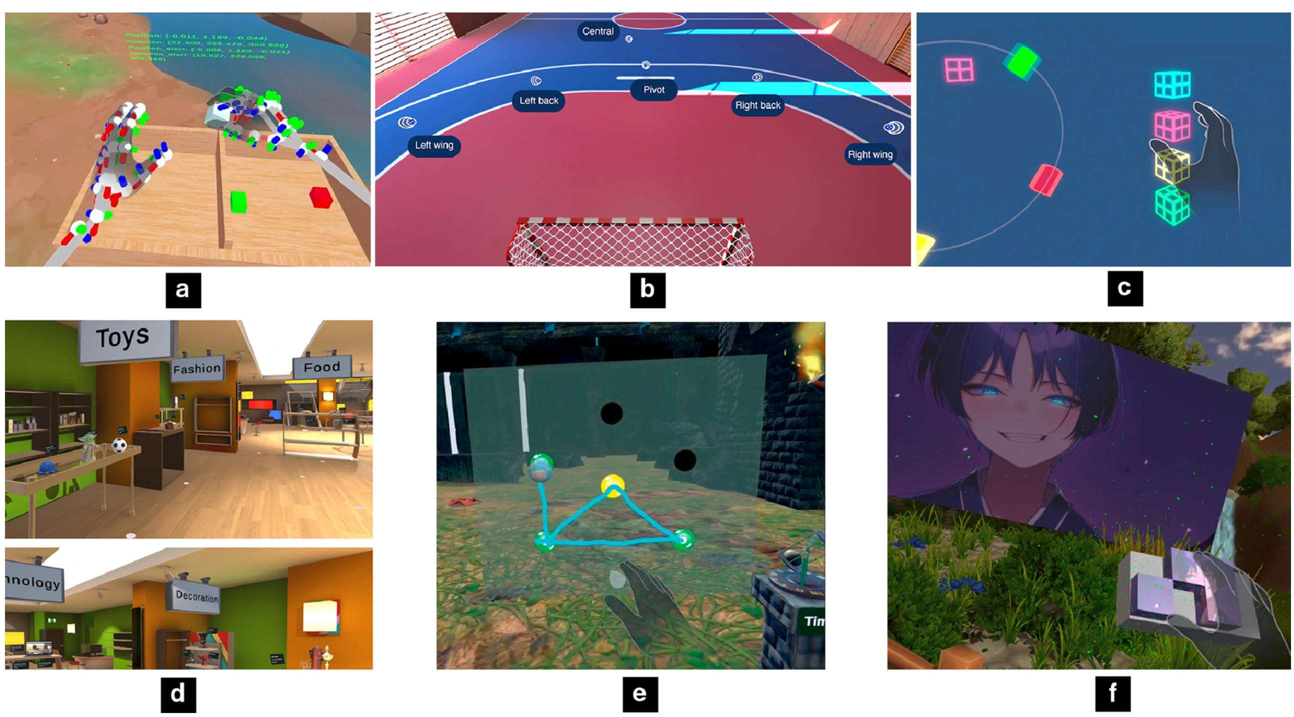

Fig. 2 Screenshots of several mini-games developed and integrated into the platform: **(a)** a virtual adaptation of the standard Box and Block Test; **(b)** arm and hand training as a virtual handball goalkeeper; **(c)** memory exercises involving color sequences and placing pieces in the correct positions; **(d)** interactive tasks within a virtual shopping environment; **(e)** hand-drawing of specific paths, and **(f)** solving 3D puzzles

adaptations specifically related to grasping mechanisms in interaction.

However, during experimentation with serious games for upper limb rehabilitation on the platform, a critical challenge emerged: ensuring the correct placement of virtual objects within PPS. This is the space that surrounds us and is within our reach (Petrizzo et al. 2023). That is, the space where the user can interact directly with objects without using external devices such as joysticks or any other kind of controller (Vlahovic et al. 2022).

To address this, some games introduced a manual positioning system for these elements or their containers. For example, in the VR adaptation of the Box and Block Test (Mathiowetz et al. 1985), patients could pre-place the box containing the cubes. However, this method presented limitations, as some patients found it difficult to effectively manipulate and place the box, sometimes requiring therapeutic intervention.

An alternative solution involved adjusting the distance of virtual objects using buttons to move them closer or further away. Although this approach mitigated some issues, it faced significant limitations: the inability to make a global adjustment that did not account for individual differences in mobility in both limbs and did not adapt the exercise intensity to the patient's specific capabilities. That is, this method did not differentiate between the mobility of the patient's right and left upper limb, nor did it allow for fine adjustments that considered the need to bring closer or move away specific elements to challenge the patient's ability for extension, flexion, and precision.

These limitations underscore the complexity of developing a fully adaptable and patient-specific VR rehabilitation environment, emphasising the need for more dynamic solutions to personalize the rehabilitation experience.

To address these challenges, it is planned to approach the problem dynamically. On one hand, by independently calibrating the workspace for the right and left lateralities of each patient, and on the other hand, by defining an algorithm for the readjustment of virtual elements based on the calibrated area and a set of parameters that allow for adaptation to the patient's capabilities, the type, and intensity of the exercise.

The final objective is to integrate these solutions into the REHAB platform, enabling their utilisation in the serious games included in the platform itself. This approach allows for the automatic adjustment of the elements with which the user must interact in their rehabilitation process, situated within the patient's ROM. This is achieved while maintaining, as far as possible, the spatial relationship between objects, including their position relative to one another and proportional distance.

4 Self-adapting immersive environments

Our proposal for the self-adaptation of immersive environments is primarily based on an asymmetric calibration process and an algorithm for detecting objects that are out of the patients' mobility range, as well as the automatic readjustment of these interactive objects in the 3D space according to the information obtained after the calibration (see Fig. 3). In particular, this contribution is located within the "Spatial Adaptation of the Virtual Environment" module of the artificial intelligence layer, as depicted in Fig. 1. The following subsections present the formalization of these processes.

4.1 Asymmetric calibration method

To identify PPS in a virtual environment, where the patient can perform exercises according to his or her limitations, it is necessary to obtain their ROM. There are different alternatives to acquire this data, such as the use of goniometers or wearable sensors (Cluster of Health and Social Sciences 2021). In our case, we propose the use of a VR-immersive HMD with hand tracking for two main reasons. First, it avoids the use of additional instrumentation on the arms and hands, which requires more time and hinders usability. Second, since it is used in immersive environments, it is natural for the calibration to be performed through the measurements obtained with the VR device itself.

However, the use of this type of device also entails a set of limitations. It is not possible to evaluate the angle of each of the joints of the upper limb, since the most precise information provided is the direct tracking of the hands. For this reason, the calculation of the ROM is also limited to the data from each hand through a set of studied movements to obtain the adequate area to reach the farthest objects in the three planes. To this end, the movement of the shoulder has been studied, guided by I. A. Kapandji's principles on

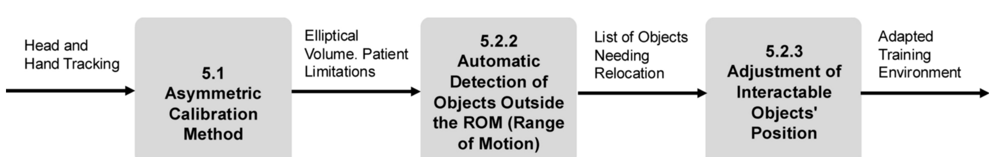

Fig. 3 General outline and simplification of input and output flows, along with the methods responsible for creating a virtual space adapted to the patient's needs

shoulder kinematics across the sagittal, frontal, and horizontal planes (Kapandji 2019).

Furthermore, to obtain an optimal calibration, it is necessary to take into account the asymmetry of the process in two senses. The ROM of the right upper limb does not necessarily coincide with the left one, and it also does not usually coincide in the horizontal and vertical planes. The multi-plane analysis can accurately capture the asymmetry in shoulder movements, which is especially noticeable in patients with SCI. This decision is supported by studies on the limitations of shoulder mobility observed in this kind of patients, who often have reduced shoulder mobility in several aspects. Specifically, in the study by Finley et al. (2020), patients had bilaterally reduced mobility in shoulder elevation, external rotation, and horizontal adduction. Therefore, separate measurements should be taken for the right and left side, also taking into account the flexion, abduction, adduction and external and internal rotation.

The following method is intended to provide a solution to the need to create a safe workspace within which the patient can comfortably perform exercises and activities without the risk of overexertion or compensatory movements that could lead to further injury or discomfort.

4.1.1 Input data for calibration method

The proposed calibration method receives as input the position and rotation of the left and right hands during a series of predefined movements, which will be described in detail in the following section. The hands and head tracking are formally defined as follows:

- $\mathrm{P}_{HMD}(t) = [P_{HMD}.x(t), P_{HMD}.y(t), P_{HMD}.z(t)]$: the position of the HMD helmet on the *x*, *y*, and *z* axes at time *t*.
- $\mathrm{R}_{HMD}(t) = [R_{HMD}.x(t), R_{HMD}.y(t), R_{HMD}.z(t)]$: the Euler angles representing the orientation of the HMD helmet around the *x*, *y*, and *z* axes at time *t*.
- For each hand, $\mathbf{P^s(t)}$ is defined, where s can be either R for the right side or L for the left side. $\mathbf{P^s(t)}$ represents the set of points obtained during the calibration, relative to the center of the palm of the hand. Each point consists of the position (*x*, *y*, *z*).The complete tracking *S*(*t*) over a time $t \in [t_0, t_f]$ is described by the set of positions P_{HMD} and rotations R_{HMD} of the HMD headset and both hands (*R* and *L*) over time P^s such that $P^s = P^R \cup P^L$:

$$\mathrm{S}(t) = \{\mathrm{P}_{HMD}(t), \mathrm{R}_{HMD}(t), \mathbf{P^s(t)}, |\ t \in [t_0, t_f]\}$$

4.1.2 Calibration method

In the processing phase, the data obtained through hand and head tracking $\mathrm{S}(t)$ are used to define a safe and personalized working area. This process responds to the needs of asymmetry between the right and left sides and differentiation between spatial planes, as discussed in the Sect. 4.1.1. To simplify the process, since what is desired is to know the maximum degree of reach without performing overexertion or compensatory movements in a virtual environment, it is not necessary to measure the angle of each joint, but rather the final position of the hand through a set of movements that cover the entire safe workspace. In this case, the ROM measurement does not include the measurement of the ROM of the set of joints individually for two reasons. The first is due to the limitations given by the HMD device and the direct tracking that allows accurate data to be obtained for the hands, unlike the arm and forearm which is done by inverse kinematics. The second reason is that the measurement of the ROM of each joint is not necessary to calibrate the safe working zone.

The asymmetric calibration process is performed by capturing sets of points related to hand position and corresponding to specific shoulder movements in the horizontal, frontal, and sagittal planes, involving movements of flexion, extension, abduction, and adduction (both horizontally and vertically). Given the biomechanics of the shoulder, the points obtained for the right and left sides aim to define an elliptical volume for each side, formed by three ellipses that cover the 3D space. An elliptical volume is used instead of a circular one because, during vertical abduction, the movement continues towards the opposite side being exercised, creating a kind of arch that accurately defines the PPS according to laterality. The elliptical volumes are generated with the elbow and wrist extended as much as possible, and are formed by three ellipses that cover the 3D space reached by the right and left upper limbs.

Initially, the patient performs a movement from an abduction position of approximately 90° in the frontal plane, extending the arm and performing a full horizontal flexion (see Fig. 4a and b). The points collected during this exercise form the set E_H^s for both the right and left sides (E_H^R and E_H^L), obtained from $P^R(t)$ and $P^L(t)$, respectively.

Subsequently, from the same starting position, the patient raises the arm to 180° of adduction (see Fig. 4c) above the head and continues the movement to the opposite side, spanning the frontal plane (see Fig. 4d). Afterwards, the shoulder moves back to the 180-degree position above the head (see Fig. 4e), and from there, the arm is brought forward and down (shoulder flexion in the sagittal plane) to the level of the hips (see Fig. 4f). This forms a kind of arch that covers

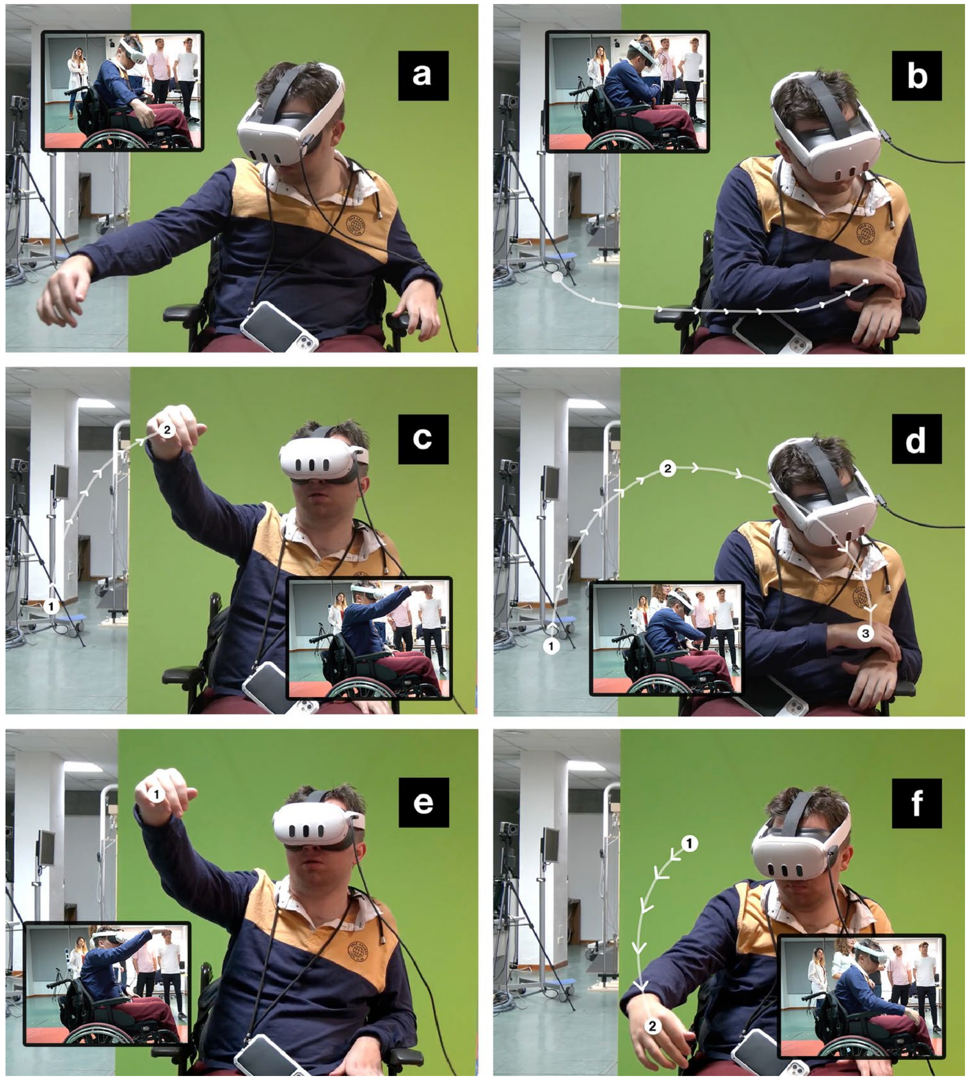

Fig. 4 Phases for the calculation of the ellipsoidal volume corresponding to the right laterality: **(a)** starting position in the horizontal and frontal plane; **(b)** final position in the horizontal plane; **(c)** intermediate position in the frontal plane; **(d)** final position in the frontal plane; **(e)** initial position in the sagittal plane; **(f)** final position in the sagittal plane

the patient, capturing the points that define the ellipses in the frontal and sagittal planes (E^s_{FS}), also obtained from $P^s(t)$.

The order of the exercises was chosen to ensure that the horizontal movement is assessed without the influence of potential fatigue from more demanding movements. The first exercise, as shown in panels (a) and (b), was selected because it does not involve shoulder abduction or significant shoulder rotation, focusing solely on horizontal displacement. In contrast, the subsequent exercises, illustrated in panels (c) through (f), require both shoulder abduction and upward rotation, which are more strenuous and can lead to greater muscle fatigue. By positioning the horizontal movement first, we ensure that this measurement is unaffected by the increased physical demands of the later exercises, allowing for a more accurate definition of the horizontal range of motion and providing precise information on reach capacity.

Once the set of points is obtained, the calibration process transforms them into the necessary data to recreate the elliptical volume (EV^s), where s can be either R for the right side or L for the left side). This includes the centers and radii of the three ellipses. The sets of points $E^s_H \leftarrow P^s(t)$ for the horizontal ellipse, and $E^s_{FS} \leftarrow P^s(t))$ that combines the frontal and sagittal ellipses are processed to derive the elliptical parameters: centers (EC^s_H, EC^s_{FS}) and radii (ER^s_H, ER^s_{FS}) that best fit the patient's shoulder movements (see Algorithm 1).

$$
\begin{array}{l}
\textbf{function } \textsc{CalculateEllipticalParameters}(P^s_{HMD}, E^s_H, E^s_{FS}) \\
\quad EC^s_H \leftarrow \left(\frac{\max(E^s_H.x)+\min(E^s_H.x)}{2}, \frac{\max(E^s_H.y)+\min(E^s_H.y)}{2}, P_{HMD}.z\right) \\
\quad ER^s_H.x \leftarrow \max(|E^s_H.x - EC^s_H.x|) \\
\quad ER^s_H.z \leftarrow \max(|E^s_H.z - EC^s_H.z|) \\
\quad EC^s_{FS} \leftarrow \left(\frac{\max(E^s_{FS}.x)+\min(E^s_{FS}.x)}{2}, \frac{\max(E^s_{FS}.y)+\min(E^s_{FS}.y)}{2}, P_{HMD}.z\right) \\
\quad ER^s_{FS}.x \leftarrow \max(|E^s_{FS}.x - EC^s_{FS}.x|) \\
\quad ER^s_{FS}.y \leftarrow \max(|E^s_{FS}.y - EC^s_{FS}.y|) \\
\quad ER^s_{FS}.z \leftarrow \max(|E^s_{FS}.z - EC^s_{FS}.z|) \\
\quad \textbf{return } (EC^s_H, ER^s_H, EC^s_{FS}, ER^s_{FS}) \\
\textbf{end function}
\end{array}
$$

Algorithm 1 Calculation of elliptical parameters from point lists

Additionally, a base position is captured to determine the height of the knees and the width of the hips at a height defined by 90-degree flexion of the elbows. This posture is commonly used in many rehabilitation exercises. The center of the right palm and the center of the left palm (Palm Centered Position P^S_{PC}, where s can be either R for the right side or L for the left side)), are captured while the patient places their upper limbs in this manner. With these two points, it is possible to determine the position in the most centered position to the patient (*X*), at a depth (*Z*) close to the patient, and at a height (*Y*) where the objects should be placed to avoid leg interference and unnecessary trunk movement.

4.1.3 Output data for calibration method

The asymmetric calibration generates needed data for the accurate replication of the workspace tailored to each patient. This data includes the position and rotation of the HMD at the start of calibration (P_{HMD}, R_{HMD}), the coordinates of the right (P^R_{PC}) and left (P^L_{PC}) palms when the elbows are bent at 90° centered to the patient (palm center position P^s_{PC}). Furthermore, the parameters of the ellipses defined for the three principal planes are included: the horizontal plane (E^s_H) is described by the center (EC^s_H) and the radii (ER^s_H); the frontal and sagittal planes (E^s_{FS}) are characterized by the center (EC^s_{FS}) and the radii (ER^s_{FS}), where s indicates R for right and L for left.

4.2 Automatic detection and adjustment of interactive objects

The aim of these methods is to adapt the immersive environment to the patient's ROM. In this way, the virtual elements that the user manipulates directly will always be within his or her PPS, either in their entirety or in a specific area of the PPS (see Fig. 5). This safe working area is obtained through the previous calibration process, which is part of the data input.

As with the calibration method, the asymmetry of right and left movements must be taken into account in the environmental adaptation methods. Not only because the ROM of one side or the other may be different within the same

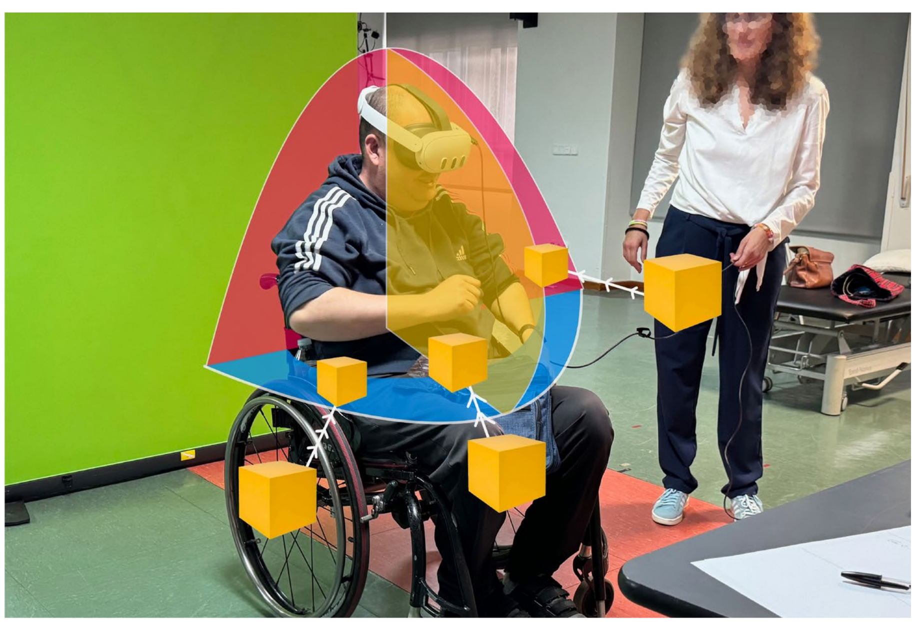

Fig. 5 Elliptical volume defined for right laterality and relocation of elements in the virtual space according to this volume

patient, but also because the area in which the exercises are performed must be configurable. It is important to bear in mind that rehabilitation exercises may be mono-manual or bimanual (Anderson et al. 2019), may require lateral movements of the trunk or, conversely, may be performed with the trunk in a static position. Furthermore, the intensity of the exercise must be adjustable in terms of the position of the elements. This last aspect refers to the position of the elements within the patient's ROM at different distances in order to modify the intensity of the exercise.

4.2.1 Input data

The methods for detecting and readjusting virtual elements in an immersive environment share the same input data. This data is categorized into three types: i) the output data obtained from the calibration process, ii) the configuration parameters tailored to the type of exercise being performed, and iii) the set of virtual objects to be analyzed and possibly relocated.

First, the input parameters are obtained from the calibration output (see Sect. 4.1.3). Second, the parameters related to exercise configuration are necessary for replicating the working area. The processes adopt a set of configurable input parameters to adapt to the intensity and type of exercise. Among these parameters is the zone within the calibrated area where the exercise will be performed: central zone, right lateral zone, left lateral zone, and global zone (see Fig. 6). The central zone (Z_C) is the area corresponding to the frontal part of the patient that spans the width of their body. This zone can be applied to both monomanual and bimanual exercises. On the other hand, the right lateral zone (Z_R) is for exercises with the right upper limb, and the left lateral zone (Z_L) is for monomanual exercises with the left hand. Lastly, the global zone includes all three areas (Z_G), used for bimanual exercises, as it encompasses the central zone as well as the lateral zones reachable by the upper limbs (left or right). In addition to the designated areas, a patient-centered point, called the *central point of coincidence* (P_{CPC}), is considered for the location of the virtual targets. This is a position widely used in various rehabilitation exercises to place the elements directly in front of the patient and centered on the patient, at a height above the knees.

Among the parameters related to exercise configuration, there are settings intended to adapt the intensity and type of exercise to be performed. These include a threshold and a height restriction. The threshold refers to the calibrated lateral areas for the right and left sides (Z_R and Z_L). The area threshold, expressed as a percentage (T_Z), adjusts the extent of the lateral zones in relation to the calibrated area. It can be set at 100% to use the entire calibrated area, reduced to less than 100% for a smaller work area, or expanded to more than 100% for a larger area. With this threshold, it is possible to modify the exercise intensity since an area close to 100% requires more effort from the patient compared to a reduced area (less than 100%).

Additionally, an input parameter is defined regarding the height restriction. The height restriction parameter ($H_{\text{Restriction}}$) determines if there is a minimum height constraint (H_{Limit}) for placing objects within the virtual environment. Thanks to this parameter, it is possible to adapt the exercise according to whether lateral trunk displacement is required. If the height restriction is not active ($H_{\text{Restriction}} = \text{false}$), the height constraint is removed, allowing objects to be placed below the height corresponding to the height of the legs, thus permitting lateral trunk movements. Conversely, if the height restriction is active ($H_{\text{Restriction}} = \text{true}$), the minimum height constraint is enforced for object placement.

This height restriction is a configurable parameter, with the exception of cases where the x-coordinate of the geometric center of the virtual object ($P_{\text{VO}}.x$) is within the interval defined between the x-position of the center of

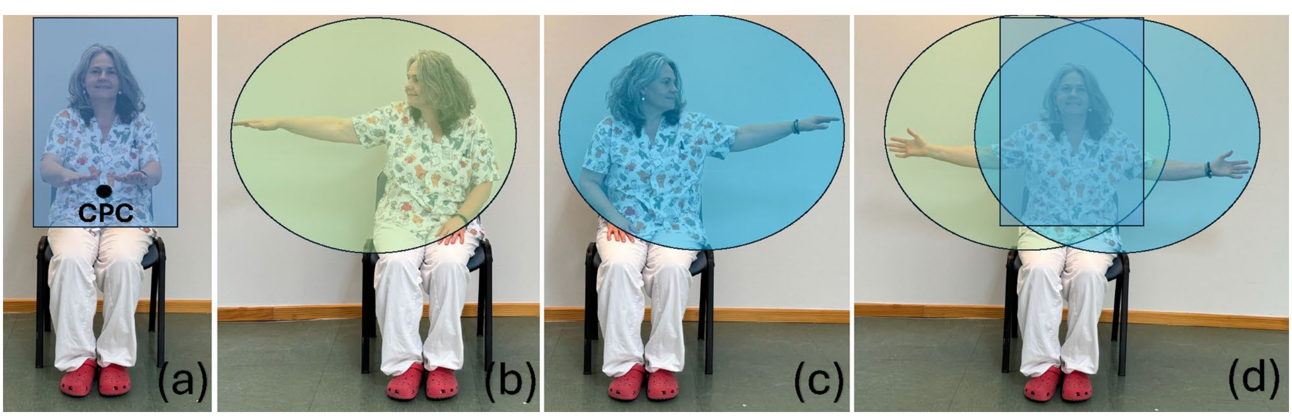

Fig. 6 Configurations of the workspace for automatic detection and adjustment algorithms. From right to left: **(a)** central zone (Z_C) and central point of coincidence (P_{CPC}); **(b)** right lateral zone (Z_R); **(c)** left lateral zone (Z_L) and **(d)** global zone (Z_G)

the right palm and left palm ($P_{\mathrm{PC}}^{R}.x$ and $P_{\mathrm{PC}}^{L}.x$). This is because within this x-interval, the patient's legs are located, as the exercises are performed in a seated position. Therefore, no virtual object can be placed below this height.

Third, the input parameters include a list of virtual objects (VO), denoted as $\mathcal{L}_{\mathrm{VO}}$. Each of these objects includes details about the 3D position, namely its geometric center, the volume of the object, marker to determine if relocation is necessary, the new position if it is necessary, and whether the relocation was successful. The latter is because the relocation process tries to move the object if necessary and if possible, i.e. if the object does not fully or partially collide with another object already positioned and if it is within the configured area. Since virtual objects can have different shapes, a dodecahedron is used to enclose the virtual object in order to unify calculations. The components of each VO are specified as follows:

$$\mathcal{L}_{\mathrm{VO}} = \{(P_{\mathrm{VO}}, V_{\mathrm{VO}}, S_{\mathrm{VO}}, NP_{\mathrm{VO}}, R_{\mathrm{VO}}) \mid P_{\mathrm{VO}} \in \mathbb{R}^3, V_{\mathrm{VO}} \in \mathbb{R}^3, S_{\mathrm{VO}} \in \{0,1\}, NP_{\mathrm{VO}} \in \mathbb{R}^3, R_{\mathrm{VO}} \in \{0,1\}\}$$

where P_{VO} is the central geometric position, V_{VO} is the volume defined as (L_x, L_y, L_z) representing the dimensions of the dodecahedron along the x, y, and z axes, S_{VO} is the status flag (1 if correctly positioned, 0 otherwise), NP_{VO} is the new calculated geometric position if the object needs to be relocated, and R_{VO} is the relocation status flag (1 if successfully relocated, 0 otherwise).

4.2.2 Automatic detection of interactable objects outside the PPS

Before the automatic detection and adjustment algorithms begin, the calibrated area is corrected based on the current HMD position ($P_{\mathrm{CurrentHMD}}$) and the applied threshold for area (T_Z). This pre-adjustment ensures that the calibration data is adapted to any changes in the user's position or system configuration.

This presetting ensures that the calibration data adapts to any changes in the user's position or in the system configuration. To do so, it is necessary to modify the data concerning the ellipsoidal volumes (EV^s), defined as the volume formed by the ellipses (E_H^s, E_F^s, and E_S^s), and the palm center positions for the right and left sides (P_{PC}^s) based on the difference between the P_{HMD} obtained during calibration and the current $P_{\mathrm{CurrentHMD}}$. After this, the radii and centers of the ellipsoidal volumes are modified according to the threshold (T_Z), whether it is greater or less than 100%. As can be seen, this threshold does not affect the palm center positions since these points are calculated from a very specific position (described in Sect. 4.1.2) that should not be varied, as they indicate the minimum height at which objects should be placed (otherwise they would interfere with the legs), the x-range occupied by the patient's body (height of the hips), and the optimal depth with elbows flexed at 90°. After this pre-adjustment, the input data are modified accordingly to the output data of the calibration (including the radii ER_H, ER_F, ER_S and centers EC_H, EC_F, EC_S, as well as the palm center positions P_{PC}^{R} and P_{PC}^{L}).

After the initial pre-adjustment, the detection process begins by checking the height restriction ($H_{\mathrm{Restriction}}$). It is important to note that this restriction is configurable, except when the x-coordinate of the object falls within the range defined by the interval $[P_{\mathrm{PC}}^{R}.x, P_{\mathrm{PC}}^{L}.x]$ (i.e., $P_{\mathrm{VO}}.x \in [P_{\mathrm{PC}}^{R}.x, P_{\mathrm{PC}}^{L}.x]$). In this case, as explained in 4.2.1, regardless of the input configuration, the height restriction will be maintained. If the height restriction is active, it is verified that the object's y-coordinate does not exceed the height limit. To determine this, it is first necessary to calculate P_{CPC}, which is the average of P_{PC}^{R} and P_{PC}^{L} ($P_{\mathrm{CPC}} = \mathrm{average}(P_{\mathrm{PC}}^{R}, P_{\mathrm{PC}}^{L})$) (see CheckHeightRestriction function in Algorithm 2). Consequently, the height limit is defined as $H_{\mathrm{Limit}} = (P_{\mathrm{CPC}}.y)$.

After verifying the height (y) of the virtual object (P_{VO}), the process continues by detecting whether the object is outside the zone established in the configuration (Z_R, Z_L, Z_G) or if it corresponds with the central point of coincidence (P_{CPC}). For the case of the right (Z_R) or left (Z_L) zone, it is checked that the geometric center is within the ellipsoidal volume of the right or left side, as appropriate (see Algorithm 2). The division of elliptical volumes (EV^s) simplifies calculations. Thanks to the biomechanics of the shoulder, at 90° of flexion in the sagittal plane, the humeral head is in an optimal position. This allows a greater range in depth (Z-plane) because there is sufficient space between the humeral head and the glenoid cavity (Chang et al. 2024). If the object is in the horizontal plane and below the height corresponding to the center of the frontal and sagittal ellipses ($P_{\mathrm{VO}}.y \leq EC_{FS}.y$) and above the point considered as central, the object is within the area if it lies within the horizontal ellipse ($P_{\mathrm{VO}}.y < H_{\mathrm{Limit}}$). Otherwise, it should be checked within the ellipses defined in the sagittal and frontal planes (E_F and EC_S). For the global zone (Z_G), it is checked that the center of the ellipsoidal volume is either within the volume defined for the right (Z_R) or left (Z_L) lateral zone ($Z_G = Z_R \cup Z_L$).

In the case of the central zone (Z_C), it evaluates whether the object is within the x and y range defined by the positions of the palms of the hands ($P_{\mathrm{VO}}.x \leq (P_{\mathrm{PC}}^{R}.x)$ and $P_{\mathrm{VO}}.x \geq (P_{\mathrm{PC}}^{L}.x)$), and additionally, whether it is contained within any of the ellipses of the side zones. Given the characteristics of the central zone, where the patient's legs are located, it also determines whether the y position of NP_{VO} is greater than or equal to H_{Limit} ($NP_{\mathrm{VO}}.y \geq H_{\mathrm{Limit}}$).

Finally, for the central point of coincidence (P_{CPC}), it is identified whether the object occupies exactly the point calculated from the arithmetic mean of the palm positions, ensuring a centered positioning relative to the user ($P_{\mathrm{CPC}} = \mathrm{mean}((P^R_{\mathrm{PC}},\ P^L_{\mathrm{PC}})$. For the side zones ($Z_L$ and Z_R), the algorithm determines whether the object's position is contained within the corresponding ellipses (E_H, E_F, E_S). For the global zone (Z_G), which includes both side zones, it verifies that the object is inside at least one of the side ellipses.

After the detection process is completed, each of the virtual objects (P_{VO}) in the list of objects ($\mathcal{L}_{\mathrm{VO}}$) detected outside the defined area is marked for subsequent relocation (S_{VO}).

object is successfully relocated, the relocation flag (R_{VO}) is set to 1.

In this algorithm, the collision area of an object with another, understood as an orthohedron that contains the virtual object (V_{VO}), is also taken into account. Therefore, it is possible that an element cannot be relocated even if a position within the specified working area is found, if it collides with any of the objects that do not require relocation or that have already been relocated so far.

The readjustement process starts by processing the list of virtual objects $\mathcal{L}_{\mathrm{VO}}$ to identify those that need relocation. Each object marked as $S_{\mathrm{VO}} = 0$ is processed by the dynamic realignment algorithm to assign it a new position considering the calibration data and the set configuration. For each object requiring relocation, its original position

function $\textsc{DetectAndMarkObjectsOutsideZones}(\mathcal{L}_{\mathrm{VO}}, Z_{\mathrm{area}}, H_{\mathrm{Limit}}, H_{\mathrm{Restriction}})$
  for each $(P_{\mathrm{VO}}, V_{\mathrm{VO}}, S_{\mathrm{VO}}) \in \mathcal{L}_{\mathrm{VO}}$ **do**
    $S_{\mathrm{VO}} \leftarrow \mathrm{CheckHeightRestriction}(P_{\mathrm{VO}}, H_{\mathrm{Limit}}, H_{\mathrm{Restriction}}, P^R_{\mathrm{PC}}, P^L_{\mathrm{PC}})$
    if $S_{\mathrm{VO}} \neq 0$ **then**
      $S_{\mathrm{VO}} \leftarrow$
      if $Z_{\mathrm{area}} == Z_C$ **then**
        $P_{\mathrm{VO}}.x \geq P^R_{\mathrm{PC}}.x$ and $P_{\mathrm{VO}}.x \leq P^L_{\mathrm{PC}}.x$ and $(\mathrm{IsWithinEllipse}(P_{\mathrm{VO}}, Z_R)$ or $\mathrm{IsWithinEllipse}(P_{\mathrm{VO}}, Z_L))$
      else if $Z_{\mathrm{area}} == Z_G$ **then**
        $(\mathrm{IsWithinEllipse}(P_{\mathrm{VO}}, Z_R)$ or $\mathrm{IsWithinEllipse}(P_{\mathrm{VO}}, Z_L))$
      else if $Z_{\mathrm{area}} == Z_PCC$ **then**
        $(P_{\mathrm{VO}} == P_{CPC})$
      else
        $\mathrm{IsWithinEllipse}(P_{\mathrm{VO}}, Z_{\mathrm{area}})$
      end if
    end if
  end for
end function
function $\textsc{CheckHeightRestriction}(P_{\mathrm{VO}}, H_{\mathrm{Limit}}, H_{\mathrm{Restriction}}, P^R_{\mathrm{PC}}, P^L_{\mathrm{PC}})$
  $heightRestriction \leftarrow H_{\mathrm{Restriction}}$ or $(P_{\mathrm{VO}}.x \geq P^R_{\mathrm{PC}}.x$ and $P_{\mathrm{VO}}.x \leq P^L_{\mathrm{PC}}.x)$
  if $heightRestriction$ and $P_{\mathrm{VO}}.y \leq H_{\mathrm{Limit}}$ **then**
    return 0
  else
    return 1
  end if
end function

Algorithm 2 Detect and mark objects for relocation

4.2.3 Automatic object adjustment and creation of an adapted and accessible environment

Upon completing the detection phase, the automatic adjustment algorithm initiates the process of assigning new positions to objects identified as inaccurately positioned. Using recalculated coordinates and applied thresholds, this algorithm determines the new position NP_{VO} within the designated working area for each object. Taking into account height restrictions and exercise zone specifications. If the

P_{VO} is assigned to the new position variable (NP_{VO}). The algorithm then works with NP_{VO}.

The first adjustment concerns the height constraint. In a similar way to the detection process (CheckHeightRestriction function in Algorithm 2), if it is detected that the object is outside the y-coordinate constraints, then it is adjusted to the height limit ($NP_{\mathrm{VO}}.y = H_{\mathrm{Limit}}$).

Once the y-coordinate is adjusted, the algorithm checks if the object needs further relocation by verifying if it is within the selected area. If this modification satisfies the inclusion of the object in the selected area and it does not collide with any other element, the next object is processed. Otherwise, the algorithm proceeds to relocate it according to the working area. This provides a potential position for the geometric center of the virtual element within the defined area. However, it may happen that the volume of the object collides, wholly or partially, with another virtual object that does not require relocation or with any of the objects relocated so far. To increase the flexibility of the algorithm, it analyses if there is a collision. In such a case, it progressively decreases the threshold of the calibrated area to search for a new point that satisfies the conditions. This process continues until a position is found that meets the area and collision restrictions or until any of the orthohedron's faces have an x-coordinate less than the z-position of the current HMD ($P_{\mathrm{CurrentHMD}}$), which indicates the current z-position of the patient (see Algorithm 3).

For the calculation of the new position after verifying the y-position and the virtual object ($NP_{\mathrm{VO}}.y$), the configured area (Z_R, Z_L, Z_C, Z_G) is taken into account, or if relocation to the central point of coincidence (P_{CPC}) is required. The algorithm *CalculateNewPositionByArea* is described as follows:

- *Right area* (Z_R): the algorithm searches for a point within the right elliptical volume (EV^R)). Refer to the function AdjustToEllipse in Algorithm 4.
- *Left area* (Z_L): for the left area, the algorithm similarly searches for a point within the left elliptical volume (EV^L)). Refer to the function AdjustToEllipse in Algorithm 4.
- *Global area* (Z_G): the algorithm checks if NP_{VO} is within the elliptical zones of either Z_R or Z_L. If not, it calculates the projected point in the right (EV^R)) and

```
Input: List of virtual objects L_VO)
Output: Updated positions and relocation flags for virtual objects
for each (P_VO, V_VO, S_VO, R_VO) ∈ L_VO do
    NP_VO ← CalculateNewPositionByArea(P_VO)
    T_Z ← 100%
    R_VO ← false
    while T_Z ≥ 10% do
        collision ← CheckForCollisions(NP_VO, L_VO)
        if no collision then
            R_VO ← true
            break
        else
            T_Z ← T_Z − 5%
        end if
    end while
end for
```

Algorithm 3 CheckCollision

```
function AdjustToEllipse((NP_VO, Z_area)
    (EC_H, ER_H, EC_FS, ER_FS) ← GetEllipseParameters(Z_area)
    if (NP_VO.y > EC_FS.y then
        if not IsWithinEllipse((NP_VO, Z_area) then
            (NP_VO ← FindPointOnEllipse((NP_VO, EC_FS, ER_F, 'F', ER_S, 'S')
        end if
    else
        if not IsWithinEllipse((NP_VO, Z_area) then
            (NP_VO ← FindPointOnEllipse((NP_VO, EC_H, ER_H, 'H', ER_S, 'S')
        end if
    end if
    return NP_VO
end function
function FindPointOnEllipse(P, C, R_1, axis1, R_2, axis2)
    angle ← arctan( (P[axis2] − C[axis2]) / (P[axis1] − C[axis1]) )
    return (C[axis1] + R_1 cos(angle), C[axis2] + R_2 sin(angle))
end function
```

Algorithm 4 Calculate new position for virtual object

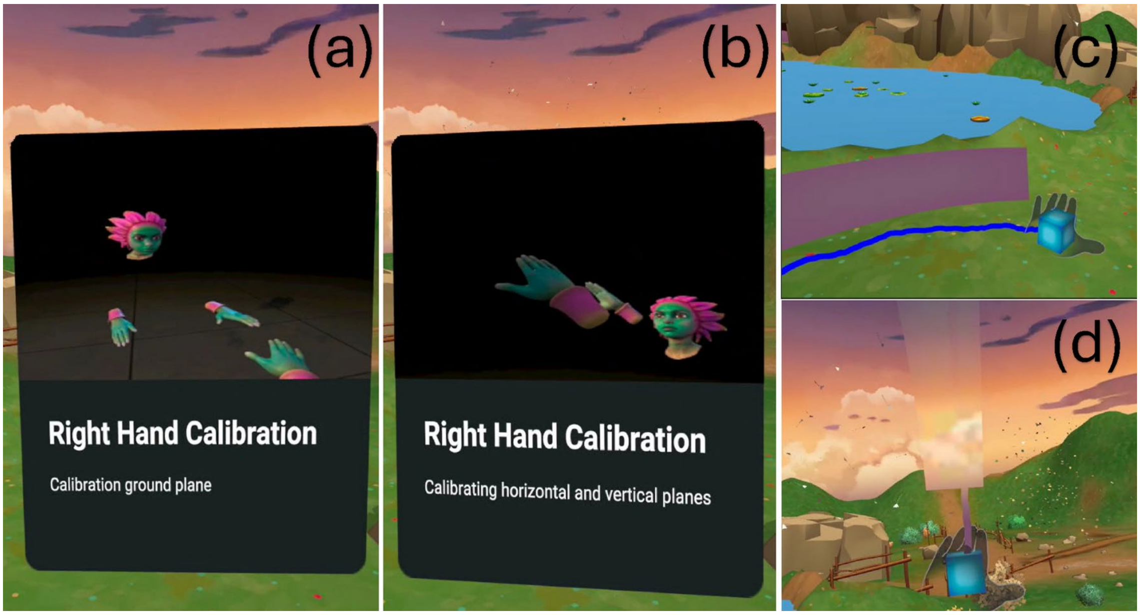

Fig. 7 Images of the visual guidance provided during the calibration process: snapshot of the pre-calibration explanatory videos to obtain E_H^R (**a**), and $E_F S^R$ (**b**); calibration tracking guide (semi-ellipse) and line drawn in the virtual environment according to hand tracking in the horizontal (**c**) and sagittal planes (**d**) for left laterality

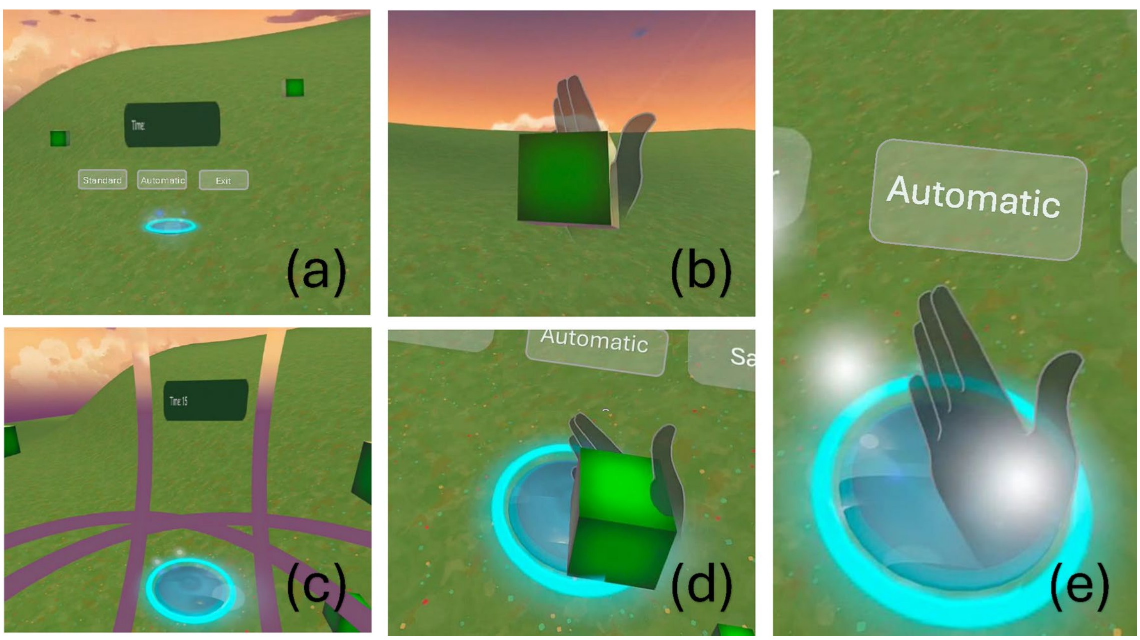

Fig. 8 Properties of the immersive VR environment designed to test the detection and automatic adjustment algorithms: **(a)** gravity-deficient cubes; **(b)** auto-attachment mechanism; **(c)** visual assistance; **(d)** target surface placement; **(e)** audiovisual aid for release

left (EV^L)) elliptical volumes. The new position is assigned to the point with the shortest distance between NP_{VO} and the calculated points. Refer to the function AdjustToEllipse in Algorithm 4.

- *Central area* (Z_C):
  - First, it checks if the x-coordinate of NP_{VO} is outside the central range. If so, it searches for the nearest point within the x-range defined by the palms of the hands $[P^R_{\mathrm{PC}}.x, P^L_{\mathrm{PC}}.x]$. If the x-coordinate is within range, no adjustment is made to x.
  - The algorithm then calculates the points that delimit the right volume (EV^R)) and the left volume (EV^L)). It assigns the new position to the point with the

shortest distance between NP_{VO} and the calculated points of the ellipses. Refer to the function AdjustToEllipse in Algorithm 4.

- *Central point of coincidence* (P_{CPC}): the new position is assigned to the calculated central point, $NP_{\mathrm{VO}} \leftarrow P_{\mathrm{CPC}}$.

5 Experimentation and results

To evaluate the effectiveness and adaptability of the calibration, automatic detection of objects out of range, and adjustment algorithms developed for upper limb rehabilitation in patients with SCI, a dedicated immersive VR environment was designed. This specialized environment was developed with the input from SCI specialists to ensure that it meets the therapeutic needs of the patients. It is designed to test the data obtained from the calibration process and to use these data as inputs for the detection and readjustment algorithms.

Both the calibration process and the detection and readjustment algorithms have been implemented using Unity (V2022.3.16f1), together with Meta XR All-in-One SDKV62. The algorithms described in this paper were implemented using the C# programming language. In addition, it has been complemented with the core developed in Rehab-Immersive that allows to capture and store kinematics of the upper limbs during the execution of the exercise (Herrera et al. 2023).

5.1 Preparation of the environment

In order to facilitate the calibration process and prevent potential errors, the environment has been prepared to guide the process, with division into stages and the incorporation of a variety of aids. These include the incorporation of pauses to prevent fatigue and the pre-explanation of each phase through a video in which a virtual avatar performs the necessary movements for the patient (Fig. 7.a and 7.b). In addition, a minimalist natural space has been recreated to provide a calm and relaxing environment for exercise. Finally, auditory and visual feedback provides additional assistance to the user from the beginning to the end of the process.

The data collected during the calibration process (explained in Sect. 4.1.1) are produced in several phases. During data acquisition, it is essential to perform all movements with a straight back, proper support, and without torso twists or compensations. Initially, the HMD position (P_{HMD}) is recorded while the user looks straight ahead. Next, data from the palms (P^{R}_{PC} and P^{L}_{PC}) are collected with the user's elbows flexed at 90°, hands above the legs, and at hip width. Subsequently, ellipses in the frontal, sagittal, and horizontal planes for the right side (E^{R}_{H}, $E_{F}S^{R}$) are obtained.

Given the complexity of this phase, a visual aid is displayed alongside the user's movements. The aid takes the form of a semi-ellipse corresponding to the plane being calibrated (Fig. 7c and d). Additionally, a cube is attached to the user's hand, tracking their task in the virtual space. After completing this phase, the formed ellipses are shown, and another cube appears attached to the palm. This time, the cube changes color-green if the hand is within the calibrated space and red if it moves outside (a demonstration of the bilateral calibration process can be viewed at https://youtu.be/RK2OOUt5aOw&t=22s).

Once verification is complete, the process is repeated for the left upper limb (E^{L}_{H}, $E_{F}S^{L}$). The calibration concludes by storing the algorithm's output information in a *JSON* file. This cumulative *JSON* file tracks the patient's ROM at different rehabilitation stages.

To evaluate the suitability of the calibration process and the use of the obtained data to detect and relocate virtual elements outside the acquired PPS, a virtual environment has been designed for this purpose. In this VR environment, five cubes are displayed in various positions within a 3D space. The participant is required to move all possible cubes

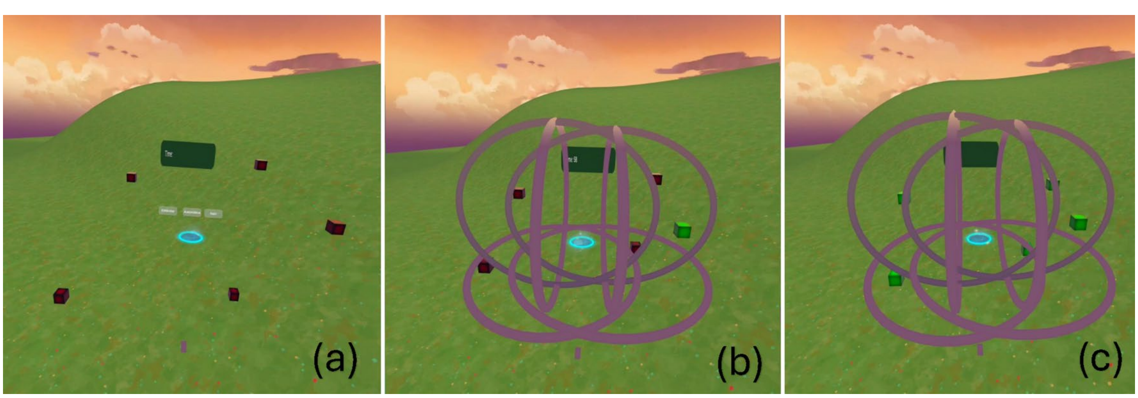

Fig. 9 Virtual environment used for testing the automatic adjustment process. From left to right: **(a)** blocks in fixed position; **(b)** standard setting and elliptical volume; **(c)** automatic setting and elliptical volume

from their initial positions to a central point located directly in front of them. This task is designed to be completed without overexertion or movements that might pose a risk to the patient's health. Notable aspects of this VR environment include:

- *Gravity-deficient cubes*. The virtual space hosts five cubes devoid of gravity, allowing for their placement in any position within the X, Y, and Z coordinates. This feature ensures the flexibility required to test the range of motion and interaction capabilities of the user (Fig. 8a).
- *Auto-attachment mechanism*. To ensure that the test focuses on environmental adaptation, specifically in terms of the positioning of virtual elements and minimizing biases related to the patient's manipulative dexterity, the cubes in the virtual environment are equipped with an *automatic grasp* mechanism (Fig. 8b). This feature automatically attaches the cube to the user's hand when it comes into contact with the object's volume. The cube remains attached until it approaches the target surface. Similarly, the action of releasing the cube does not require finger movements, as it automatically detaches after a brief period of 1.5 seconds upon reaching its destination. This setup ensures that the evaluation concentrates on the effectiveness of the environmental adjustments to meet the specific needs of the user, independent of manual skill.
- *Visual assistance*. Prior to attempting to grasp the cube, visual cues indicate whether it is within the delimited workspace based on the user's ROM. Cubes appear in red if they are outside this area and green if they are within it (Fig. 8c).
- *Target surface placement*. The target surface where the cube should be deposited is positioned centrally to the user and close to their trunk, ensuring ergonomic placement that minimizes strain (Fig. 8d).
- *Audiovisual aid for release*. When a cube remains on the target surface during 1.5 s, indicating it should be released, a sound is emitted, the cube disappears and particle effects are displayed to indicate the status of the grasp release (Fig. 8e).

5.2 Test configuration and quantitative metrics

The evaluation is performed in a virtual environment in which three different configurations are shown to test the effectiveness of the calibration, automatic detection and adjustment algorithms under different conditions: *fixed configuration*, *standard configuration* of a healthy participant and *automatic configuration*.

The *fixed configuration* consists of placing the cubes in a fixed, standard layout regardless of the individual's ROM (see Fig. 9a). This arrangement of virtual objects was previously tested in a pilot test with healthy participants, revealing that, although the cubes were reachable, reaching them often required excessive elbow extension, trunk movements and even frontal and lateral displacements, sometimes forcing participants to get up from their chairs.

With the second configuration, *standard configuration*, although it employs the detection and automatic adjustment algorithms, it does not rely on the calibration of the user testing the virtual environment (see Fig. 9b). Instead, it utilizes data calibrated based on an average individual. Specifically, calibration data from a middle-aged participant without mobility issues and with an approximate height of 166 cm was used for this purpose. This configuration assesses the user's interaction with the cubes within a standardized area, offering insights into their reach capabilities in comparison to the average individual.

Finally, the *automatic configuration*, the cubes are dynamically adjusted according to the specific calibration data of the participant being evaluated in the virtual environment (see Fig. 9c). This configuration evaluates the user's ability to interact with the cubes within an area adapted to their own ROM and mobility constraints. By using the calibration data obtained during the initial setup phase, this scenario provides a personalized assessment of the user's reach capabilities and rehabilitation progress within the virtual environment.

It is important to note that in both the second and third configuration, the ellipses defining the calibrated workspace of the test user are displayed. Given that the first and second configurations are not customized to accommodate the participant's ROM, there exists the possibility that the cubes may be displayed in red, signifying their placement beyond the bounds of the participant's workspace.

The quantitative metrics employed to assess adaptation and interaction within the VR environment are designed to capture both the displacement of objects in 3D space and the adequacy of their placement within the calibrated area, as well as the task-specific measures.

Euclidean distance. This metric quantifies the displacement needed for each object. Two distances will be considered for each participant. First, the distance from the original position of each block to the position obtained after automatic adjustment, and the second defined by the distance from the standard position to the position obtained after automatic adjustment.

Additionally, to ensure the relocated virtual objects maintain the spatiality of the original data, we introduce a function for Quadrant Distribution (ϕ), which classifies the adjusted position NP_{VO} of each object into one of four defined quadrants: Q1 (upper right), Q2 (upper left), Q3 (lower right), and Q4 (lower left). The assignment to each of these quadrants depends on the object's coordinates x and y, relative to the participant. The center is defined by the x coordinate of the participant at the moment of execution ($P_{\text{CurrentHMD}}$), and the y coordinate is given by the height (H_{Limit}). This ensures that the spatial relationship is maintained considering the participant's position and height limits.

$$\phi(p) = \begin{cases} \text{Q1} & \text{if } x \geq P_{\text{CurrentHMD}}.x \text{ and } y \geq H_{\text{Limit}} \\ \text{Q2} & \text{if } x < P_{\text{CurrentHMD}}.x \text{ and } y \geq H_{\text{Limit}} \\ \text{Q3} & \text{if } x \geq P_{\text{CurrentHMD}}.x \text{ and } y < H_{\text{Limit}} \\ \text{Q4} & \text{if } x < P_{\text{CurrentHMD}}.x \text{ and } y < H_{\text{Limit}} \end{cases}$$

The metrics employed to assess adaptation and interaction within the VR environment not only measure the displacement and adjustment of objects but also focus on task performance outcomes.

First, determine whether the task has been successfully completed in all three configurations (Task Completion). Also, it is necessary to measure whether the set task has been successfully completed or not. With the Number of Blocks Moved (N_{moved}) counts the total number of blocks that participants have attempted to move, providing a measure of participant engagement and interaction with the environment.

Regardless of whether the task has been completed, the Temporal Efficiency evaluates the time efficiency of task execution. It is defined as the total time taken until the last block is moved divided by N_{moved}.

$$\text{Temporal Efficiency} = \frac{T_{\text{total}}}{N_{\text{moved}}}$$

Where T_{total} is the total time from the start of the task to the movement of the last block to the destination position.

These metrics, together with a qualitative evaluation, allow the effectiveness of the VR immersive environment for rehabilitation to be assessed. In particular, focusing on both the effectiveness of the calibration and the adaptability of the environment to meet the specific needs of the user.

Table 1 Blocks moved and time taken to move the blocks in standard and automatic configurations for each participant (P: SCI patient, H: healthy participant), along with a numerical identifier

ID	Blocks moved standard	Time blocks standard (s)	Blocks moved automated	Time blocks automated (s)
H1	5	33	5	18
H2	3	19	5	17
H3	5	24	5	16
H4	5	32	5	27
H5	5	34	5	20
H6	5	22	5	17
H7	4	37	5	20
H8	5	36	5	20
H9	5	32	5	17
H10	5	33	5	19
P1	1	12	5	23
P2	5	30	5	19
P3	3	55	5	26
P4	5	59	5	25
P5	2	57	5	16
P6	1	14	5	34
P7	5	30	5	19
P8	4	46	5	31
P9	2	43	5	30
P10	5	33	5	13
P11	0	-	5	19
P12	5	35	5	22
P13	5	23	5	15
P14	5	20	5	16

5.3 Experimental procedure

The experimental study was conducted entirely at the HNPT, in 5 experimental sessions with a total of 24 participants (some moments of the experimentation can be seen at https://youtu.be/RK2OOUt5aOw, where the participants shown in the video are part of the group of SCI participants who carried out the experimentation at the HNPT). Of these, 14 participants had SCI of varying severity and were at different stages of their functional recovery. The remaining group consisted of 10 healthy subjects, all of them were HNPT staff, including biomedical engineers, rehabilitation specialists, physiotherapists and occupational therapists.

Participants ranged in age from 14 to 54 years, with an average age of 32.54 ± 12.27 years. Heights ranged from 153 cm to 187 cm, with an average height of 174.71 ± 8.61 cm. The group of patients predominantly included individuals with injuries between C5 and C7 levels with neurological classification by means of AIS (ASIA Impairment Scale) between A-D.

Importantly, the tests were conducted under expert supervision, ensuring that participants did not perform unwanted compensatory movements, trunk movements or overexertion that could compromise their safety. All participants performed the test while seated, utilizing the Meta Quest 2 headset. Healthy participants completed the tests seated in conventional chairs, while patients performed the tests in their own wheelchairs. Prior to executing the scenarios related to calibration and the automatic adjustment of elements, the HMD was recentered to ensure accurate placement of virtual elements relative to the calibrated floor level. Also, each participant was individually instructed on how to execute it to avoid errors and biases.

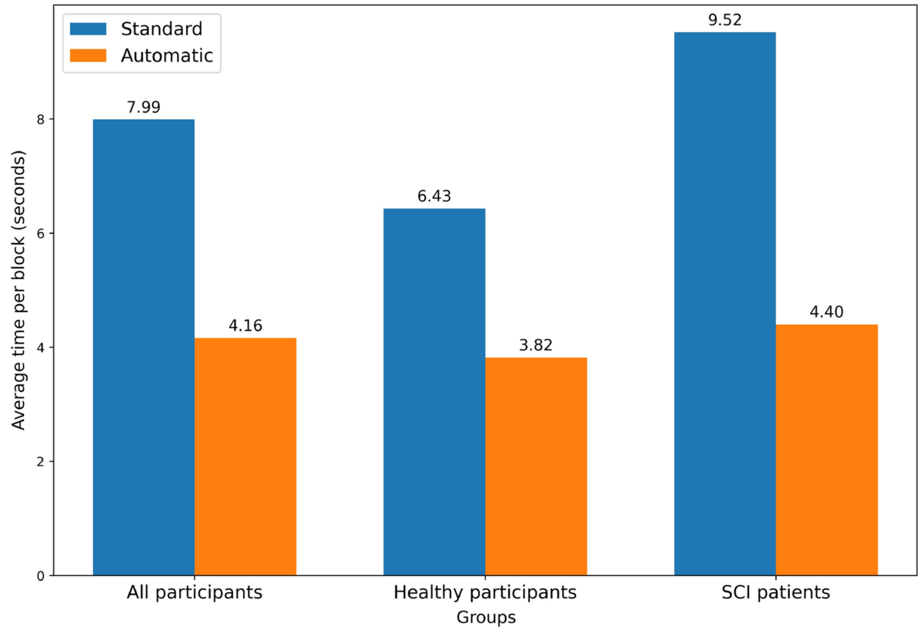

Fig. 10 Temporal efficiency measured as the average time per block in seconds for both standard and automated configurations, categorized by participant type (overall, healthy ans patient)

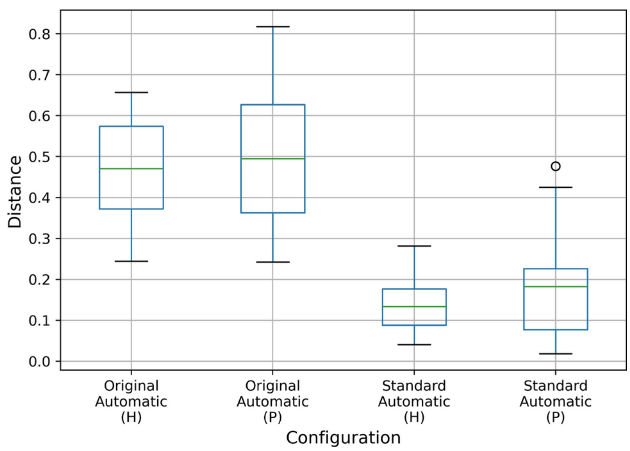

Fig. 11 Comparison of Euclidean distances across configurations. Distances are categorized by participant type (Healthy 'H' vs. Patient 'P')

Table 2 Positions in virtual space for fixed and standard configurations

Block	Fixed position (x, y, z) (*p*)	Standard position (x, y, z)
1	(−0.57, 1.0900, 0.9100)	(−0.4998, 0.9384, 0.4320)
2	(0.9900, 0.9800, 0.2000)	(0.3992, 0.9338, 0.2000)
3	(0.4500, 0.1500, 0.5000)	(0.3359, 0.7891, 0.3527)
4	(0.5700, 1.3100, 0.7100)	(0.3330, 0.9780, 0.3967)
5	(−0.9680, 0.2700, 0.2000)	(−0.5403, 0.7891, 0.1053)

Table 3 Average Euclidean distances measured in meters, standard deviations, and t-statistics

Comparison	Healthy (Avg ± SD)	Patient (Avg ± SD)
Fixed-automatic	0.4665 ± 0.1144	0.4972 ± 0.1551
Standard-automatic	0.1378 ± 0.0587	0.1721 ± 0.1057

First, each participant underwent the calibration stage, where the optimal execution method was explained to them beforehand, and their execution was supervised. The second part consisted of testing the virtual environment, where the cubes were placed according to the three configurations described. Initially, the cubes were placed in a *fixed configuration* without taking calibration into account. Due to the mobility problems of the patients, all cubes were shown in red and many of them were far away from the patients' reach. Therefore, this first part only served to check that none of the cubes could be reached by the participants and none of them were asked to try to reach the cubes, all of them being out of their ROM.

For both the second and third co-settings (standard and automatic setup), a maximum completion time of 60 seconds was set. If this time elapsed without all the cubes being placed in their destination, the test was terminated. For the second scenario (*fixed configuration*), since the ROM of a healthy subject was taken into account, participants were asked to reach only for those cubes that did not require excessive effort or trunk compensations. Those they could not reach were instructed to let the time pass. Based on the therapists' recommendations, a 5-minute rest period was provided between the two trials to eliminate any potential influence of fatigue that could affect the results.

5.4 Quantitative results

The evaluation reveals significant differences in performance between the three configurations: *fixed configuration*, *standard configuration*, and *automatic configuration*.

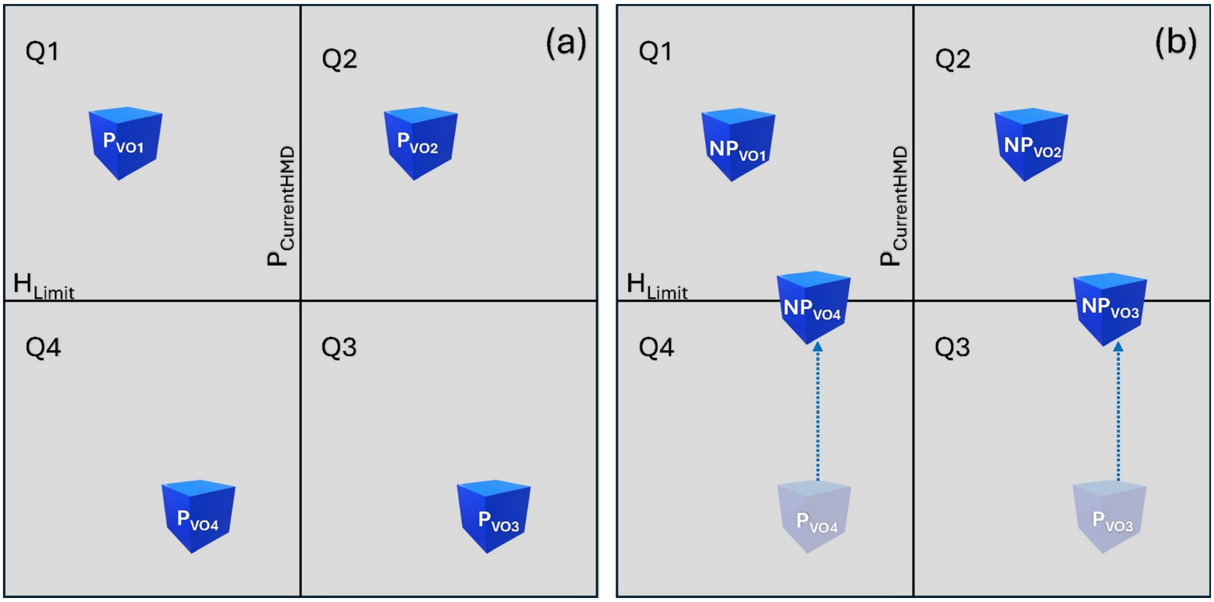

Fig. 12 Quadrant distribution (ϕ) of virtual objects. (a) original position $\phi(P_{\mathrm{VO}})$; (b) new position $\phi(NP_{\mathrm{VO}})$ after applying the automatic adjustment algorithm. NP_{VO} are relocated from quadrants Q3 and Q4 to Q1 and Q4 due to the H_{Limit}

Fig. 13 Displacement of the 5 blocks from the position set by the fixed configuration to the position defined by the automatic configuration. The values of H_{Limit} and $P_{\mathrm{CurrentHMD}}$ for the 24 participants are shown as dashed lines on the X and Y axes

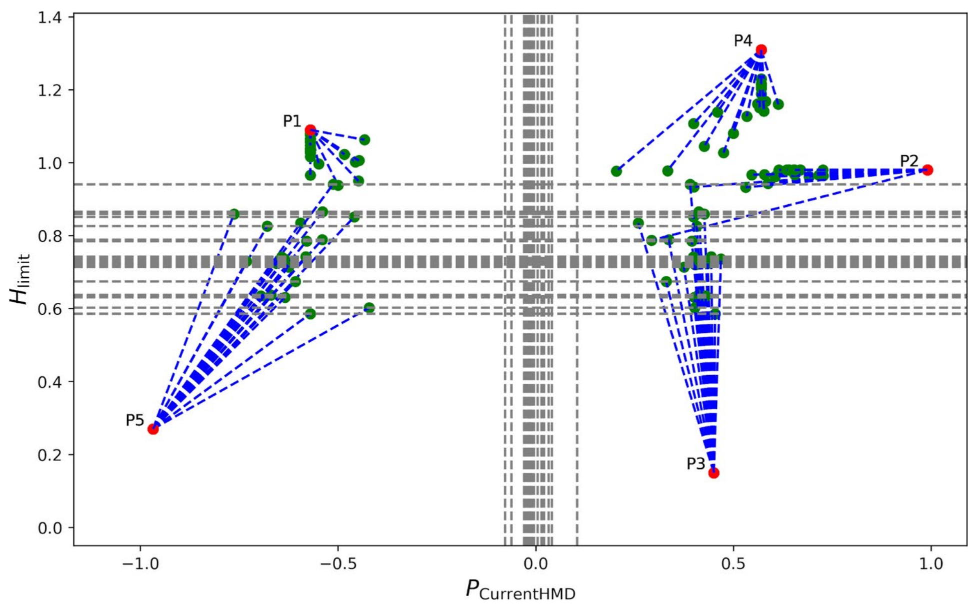

The results are presented in Table 1 and the key findings are as follows:

Task completion As previously indicated, participants were not asked to attempt to reach the blocks in the fixed configuration, as it required undesired compensations and overexertions, resulting in a 0% success rate. It is important to note that none of the participants reached the maximum time limit of 60 s for completing the task. Therefore, for those who did not finish, it was due to an inability to access the 5 blocks and not due to a lack of time. In the standard configuration, the success rate was 62.5% overall, with notable differences between healthy participants and patients. Specifically, healthy participants had a success rate of 80.0%, while patients had a lower success rate of 50.0%. Lastly, the automated mode demonstrated clear superiority, with all participants, both patients and healthy, successfully completing the task of picking up the 5 cubes and placing them in the central point, achieving a 100% success rate.

Number of blocks moved The automatic configuration showed that all participants managed to move the maximum number of blocks (5 blocks) within the allotted time. This contrasts with the standard mode, where the average number of blocks moved was significantly lower, with a mean of 3.958 for all participants, 4.7 for healthy participants, and

3.428 for patients. The *T-test* to compare differences in the number of blocks moved between healthy individuals and patients in the standard configuration revealed a *T-statistic* of 2.047 and a p value of 0.053, indicating a trend towards a significant difference that does not meet the conventional threshold for statistical significance.

Temporal efficiency The automated setup resulted in a marked improvement in temporal efficiency for all participants (see Fig. 10). Specifically, patients experienced a significant reduction in the time required per block. In standard mode, the average time per block was 7.99 seconds for all participants, 6.43 seconds for healthy participants, and 9.52 seconds for patients. With the automated configuration, this time was reduced to 4.16 seconds overall, 3.82 seconds for healthy participants, and 4.40 seconds for patients. This reduction represents a decrease of 47.94% in the average time for all participants, 40.59% for healthy participants, and 53.78% for patients.

The analysis reinforces the hypothesis that personalized adaptation of virtual environments is essential for effective rehabilitation, particularly for patients with SCI. A non-adapted environment (fixed configuration) can be entirely inaccessible or require excessive efforts and movements that may harm the user. Even considering the PPS of an average-height user (standard configuration), the results show that this is not sufficient adaptation for either patients or healthy subjects. The adaptation is even more crucial for patients, as they cannot achieve satisfactory rehabilitation if the virtual environment does not meet their needs. The conducted test reveals that calibration, automatic detection, and adjustment algorithms ensure that elements within the environment are fully accessible while minimizing times and ensuring task completion. These results validate the hypothesis that individualized configurations improve accessibility, task performance, and overall rehabilitation efficacy.

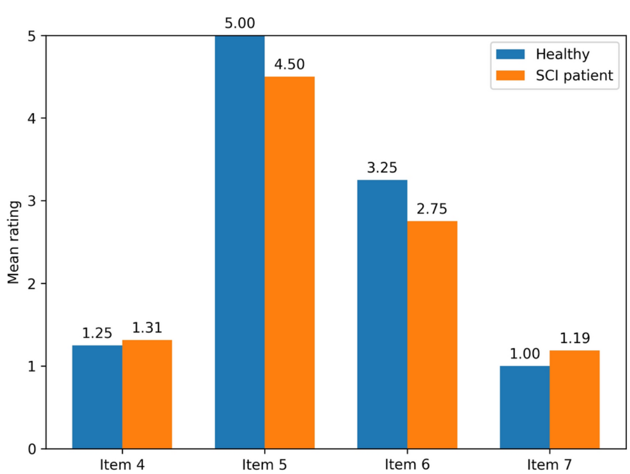

Fig. 14 Mean ratings of the questionnaire responses comparing healthy participants and SCI patients: Item 4 (calibration complexity), Item 5 (calibration adequacy), Item 6 (standard configuration complexity), and Item 7 (automatic configuration complexity)

To quantify the displacement of blocks in three-dimensional space as a function of the configuration, the Euclidean distance (measured in meters) was used to calculate the displacement from the *fixed configuration* to the *automatic configuration* and from the *standard configuration* to the *automatic configuration* (Fig. 11). It is important to note that both the fixed and standard positions are constant for all participants (Fig. 2), while the automatic position varies depending on the calibration data adapted to each participant's ROM.

Results displayed in Table 3 show that the average Euclidean distances for healthy participants were consistently lower than those for patients in all comparisons, indicating a closer alignment with the positions for healthy participants. The standard deviations were also lower for healthy participants, suggesting less variability in their movements.

For the fixed-automatic comparison, the average Euclidean distances measured were 0.4665 ± 0.1144 meters for healthy participants and 0.4972 ± 0.1551 meters for SCI patients. This suggests that healthy participants were more consistently close to the target positions, possibly indicating that these positions are better aligned with the ROM typical of healthy individuals. A t-test was conducted to assess the statistical significance of these differences, yielding a t-statistic of -1.175 and a p value of 0.242. These results indicate that the differences were not statistically significant, suggesting that the displacement from the fixed to the automatic configuration is similar for both healthy participants and patients. Consequently, the fixed configuration appears to be equally challenging or inaccessible for both groups.

However, the most relevant data come from the standard-automatic comparison. In this case, the mean Euclidean distances were 0.1378 for healthy participants and 0.1721 for patients, with standard deviations of 0.0587 and 0.1057, respectively. The t-test yielded a t-statistic of -2.063 and a p value of 0.041, indicating a statistically significant difference between the two groups. These results strongly support the hypothesis and underline the critical need for individualized calibration, especially for SCI patients, to ensure an appropriate virtual space for their ROM. Although the standard configuration fits more closely to the PPS of healthy participants, this suggests that their ROM is more consistent and predictable. However, the longer distances for patients highlight that their motor limitations make it difficult to access the blocks in the standard configuration. Therefore, the standard configuration, designed to be accessible to most people, is not well aligned with the patients' ROM, as indicated by the Euclidean distances between the standard and automatic positions.

Following the adequacy of the positioning while maintaining the spatial reference, the Quadrant Distribution ensures that the adjusted positions (NP_{VO}) of the virtual objects remain within the correct spatial configuration. The displacement of the 5 blocks from the position set by the fixed configuration can be seen in Fig. 13. For the analysis of the data, it is important to note that, due to the use of the height constraint, objects located in the automatic configuration quadrants Q3 and Q4 must be relocated to Q1 and Q2 (Fig. 12. After analyzing the data, it was confirmed that the automatic adjustment preserved the spatial arrangement within each quadrant. This consistency is evident in the data presented in Table 4.

The results show that the automatic adjustment of objects based on each participant's ROM and workspace configuration preserves spatial localisation. This ensures that items remain accessible and correctly placed within reach of the user, underscoring the effectiveness of the automatic adjustment algorithm in maintaining spatial organisation and improving accessibility for all users, particularly those with mobility impairments.

5.5 Qualitative results

To complement the results, a specific questionnaire focused on participants' perceptions of the complexity of the calibration system and its subsequent use for adjusting elements in the virtual space. The first three items collected data on the participants' age (Item 1), height in cm (Item 2), and a unique identifier to preserve anonymity (Item 3). Item 4 and item 5 are questions associated with the calibration process:

- Item 4: *did you find the automatic calibration system complex?* (5-point Likert scale where 1 means "Not at all complex" and 5 means "Very complex").
- Item 5: *after calibration, do you think the work area defined by the three ovals adequately fits the actual reach limits of your hands?* (5-point Likert scal where 1 means "Not at all" and 5 means "Completely")Item 6 and item 7 are questions that address the difficulty of accessing the blocks with standard and automatic settings, both using a 5-point Likert scale where 1 means "Not at all complex" and 5 means "Very complex":

- Item 6: *in the test after calibration, did you find it complex to access the blocks using the standard configuration?*
- Item 7: *in the test after calibration, did you find it complex to access the blocks using the automatic configuration?*The complexity of the calibration process (Item 4) was evaluated with a mean rating of 1.29 and a standard deviation of 0.46, indicating a very low perceived complexity overall. Specifically, healthy participants rated the complexity with a mean of 1.25 (SD = 0.46), while patients gave a mean rating of 1.31 (SD = 0.48).

For the calibration adjustment (Item 5), participants rated how well the calibration adapted to their reach limits. The overall mean rating was 4.67 with a standard deviation of 0.76, suggesting that the system was perceived as highly effective. Healthy participants provided a perfect mean rating of 5.00 (SD = 0.00), whereas patients rated it slightly lower, with a mean of 4.50 (SD = 0.89).

Regarding the difficulty of accessing the blocks using the standard configuration (Item 6), the overall mean rating was 2.92, with a standard deviation of 1.32, indicating a moderate difficulty level. Healthy participants had a mean rating of 3.25 (SD = 1.28), while patients rated it at 2.75 (SD = 1.34). This difference suggests that healthy participants, who were also specialists in rehabilitation, perceived the standard configuration as less accessible. This is likely because these professionals are more precise and critical about the movements required, being aware of the importance of avoiding overexertion.

Finally, for the difficulty of accessing the blocks using the automatic configuration (Item 7), the overall mean rating was 1.12 with a standard deviation of 0.45, indicating a very low difficulty level. Healthy participants rated it at 1.00 (SD = 0.00), while patients gave it a slightly higher rating of 1.19 (SD = 0.54).

To provide a visual representation of the qualitative data, the mean ratings for each aspect are depicted in Fig. 14. This bar graph shows the differences in perceived complexity and difficulty between patients and healthy participants across the three evaluated aspects.

These results, which are visually represented in Fig. 14, show the positive assessment of both the calibration and the automatic adjustment process. The perception of the participants is crucial for the success of the system, as its comfort and ease of use directly influence the effectiveness of the rehabilitation exercises. In particular, the results on the complexity of reaching the blocks in the automatic setting, very close to 1, highlight the acceptance and appropriateness of the calibrated space and the fitting algorithm. This low complexity rating underlines the effectiveness of the system in providing an accessible and user-friendly environment for both patients and healthy participants. These results support the hypothesis, confirming that individualized calibration improves accessibility and task efficiency, especially for SCI patients. The high adequacy and low complexity ratings validate the importance of personalized configurations in VR rehabilitation.

In addition, of particular importance is the inclusion of expert healthy participants, who evaluate the systems in more detail, from a more technical point of view, in terms of the appropriate movements for successful rehabilitation. These experts help ensure that the system avoids overextension and compensatory movements by defining the PPS more precisely. Their detailed assessments contribute significantly to refining the system, ensuring that it meets the standards necessary for effective and safe rehabilitation.

6 Conclusions

This study addresses the adaptation of virtual environments for upper limb rehabilitation, specifically tailored to patients with spinal cord injuries (SCI). In line with the main hypothesis, which suggests that dynamically adjusted virtual objects within a personalized 3D space calibrated to each patient's specific range of motion (ROM) will enhance task performance and safety, the system integrates automatic calibration and spatial adjustment algorithms to maintain interactive objects within the Peripersonal Space (PPS). The findings confirm that individualized configurations significantly improve task performance and efficiency, demonstrating that standard configurations-despite approximating the average ROM of a healthy individual-do not adequately support SCI patients due to their unique movement asymmetries and capabilities.

Quantitative and qualitative analyses further reveal that these personalized adjustments lead to higher task completion rates and reduce the time required per interaction, streamlining rehabilitation exercises and contributing to the prevention of compensations, overexertion, and injuries. The effectiveness of adaptive adjustments underscores the importance of calibration tailored to each patient's motor abilities, as hypothesized, highlighting their potential for creating safer and more accessible rehabilitation environments.

Future work will extend the application of these algorithms to broader clinical settings and explore their potential across diverse rehabilitation scenarios. Further research will focus on long-term impacts on functional recovery, aiming to refine and expand the system's applicability to enhance patient-centered rehabilitation outcomes.

Appendix 1: Data results

See Table 4.

Table 4 Quadrants corresponding to each of the five blocks in fixed configuration ($\phi(NP_{\mathrm{VO}})$) and automatic configuration. ($\phi(NP_{\mathrm{VO}})$). The table provides detailed information about the position of the relocated blocks NP_{VO}, the height restriction position (H_{Limit}) and the x position of the HMD at the moment of executing the adjustment ($P_{\mathrm{CurrentHMD}}$) for each participant

ID	Block	H_{Limit}	$P_{\mathrm{CurrentHMD}}$ (x)	Automatic position NP_{VO}	$\phi(p)$	$\phi(NP_{\mathrm{VO}})$
P1	1	0.7891	−0.0297	(−0.4998, 0.9384, 0.4320)	Q2	Q2
P1	2	0.7891	−0.0297	(0.3992, 0.9338, 0.2000)	Q1	Q1
P1	3	0.7891	−0.0297	(0.3359, 0.7891, 0.3527)	Q3	Q1
P1	4	0.7891	−0.0297	(0.3330, 0.9780, 0.3967)	Q1	Q1
P1	5	0.7891	−0.0297	(−0.5403, 0.7891, 0.1053)	Q4	Q2
P2	1	0.6377	0.0325	(−0.5700, 1.0656, 0.5215)	Q2	Q2
P2	2	0.6377	0.0325	(0.6408, 0.9800, 0.1025)	Q1	Q1
P2	3	0.6377	0.0325	(0.4110, 0.6377, 0.3804)	Q3	Q1
P2	4	0.6377	0.0325	(0.5700, 1.2110, 0.4807)	Q1	Q1
P2	5	0.6377	0.0325	(−0.6696, 0.6377, 0.1089)	Q4	Q2
P3	1	0.8597	−0.0264	(−0.5700, 1.0581, 0.3260)	Q2	Q2
P3	2	0.8597	−0.0264	(0.6690, 0.9800, 0.1151)	Q1	Q1
P3	3	0.8597	−0.0264	(0.4260, 0.8597, 0.4268)	Q3	Q1
P3	4	0.8597	−0.0264	(0.5700, 1.2143, 0.2731)	Q1	Q1
P3	5	0.8597	−0.0264	(−0.7631, 0.8597, 0.1172)	Q4	Q2
P4	1	0.7242	−0.0617	(−0.5700, 1.0810, 0.3799)	Q2	Q2
P4	2	0.7242	−0.0617	(0.6673, 0.9800, 0.0888)	Q1	Q1
P4	3	0.7242	−0.0617	(0.4347, 0.7242, 0.3319)	Q3	Q1
P4	4	0.7242	−0.0617	(0.5700, 1.2299, 0.3534)	Q1	Q1
P4	5	0.7242	−0.0617	(−0.6569, 0.7242, 0.0819)	Q4	Q2
P5	1	0.5861	−0.0094	(−0.4566, 1.0027, 0.5693)	Q2	Q2
P5	2	0.5861	−0.0094	(0.6908, 0.9618, 0.2000)	Q1	Q1
P5	3	0.5861	−0.0094	(0.4531, 0.5861, 0.4550)	Q3	Q1
P5	4	0.5861	−0.0094	(0.5604, 1.1609, 0.5190)	Q1	Q1
P5	5	0.5861	−0.0094	(−0.5698, 0.5861, 0.1015)	Q4	Q2

Table 4 (continued)

ID	Block	H_{Limit}	$P_{\text{CurrentHMD}}$ (x)	Automatic position NP_{VO}	$\phi(p)$	$\phi(NP_{\text{VO}})$
P6	1	0.8656	−0.0156	(−0.5488, 0.9969, 0.4763)	Q2	Q2
P6	2	0.8656	−0.0156	(0.6522, 0.9800, 0.1525)	Q1	Q1
P6	3	0.8656	−0.0156	(0.4119, 0.8656, 0.5018)	Q3	Q1
P6	4	0.8656	−0.0156	(0.5700, 1.1887, 0.4585)	Q1	Q1
P6	5	0.8656	−0.0156	(−0.5393, 0.8656, 0.1088)	Q4	Q2
P7	1	0.8511	0.0401	(−0.4482, 0.9498, 0.3110)	Q2	Q2
P7	2	0.8511	0.0401	(0.6541, 0.9676, 0.2000)	Q1	Q1
P7	3	0.8511	0.0401	(0.3987, 0.8511, 0.3318)	Q3	Q1
P7	4	0.8511	0.0401	(0.5334, 1.1274, 0.2967)	Q1	Q1
P7	5	0.8511	0.0401	(−0.4593, 0.8511, 0.0846)	Q4	Q2
P8	1	0.7874	0.0204	(−0.5700, 0.9657, 0.4114)	Q2	Q2
P8	2	0.7874	0.0204	(0.2924, 0.7874, 0.2000)	Q1	Q1
P8	3	0.7874	0.0204	(0.2591, 0.8347, 0.2571)	Q3	Q1
P8	4	0.7874	0.0204	(0.2034, 0.9770, 0.4084)	Q1	Q1
P8	5	0.7874	0.0204	(−0.5944, 0.8347, 0.1101)	Q4	Q2
P9	1	0.8263	−0.0157	(−0.5700, 1.0759, 0.4061)	Q2	Q2
P9	2	0.8263	−0.0157	(0.6515, 0.9800, 0.1021)	Q1	Q1
P9	3	0.8263	−0.0157	(0.4069, 0.8263, 0.3703)	Q3	Q1
P9	4	0.8263	−0.0157	(0.6131, 1.1600, 0.4035)	Q1	Q1
P9	5	0.8263	−0.0157	(−0.6794, 0.8263, 0.1072)	Q4	Q2
P10	1	0.5861	0.1044	(−0.4566, 1.0027, 0.5693)	Q2	Q2
P10	2	0.5861	0.1044	(0.6908, 0.9618, 0.2000)	Q1	Q1
P10	3	0.5861	0.1044	(0.4531, 0.5861, 0.4550)	Q3	Q1
P10	4	0.5861	0.1044	(0.5604, 1.1609, 0.5190)	Q1	Q1
P10	5	0.5861	0.1044	(−0.5698, 0.5861, 0.1015)	Q4	Q2
P11	1	0.9409	−0.0113	(−0.5700, 1.0803, 0.3834)	Q2	Q2
P11	2	0.9409	−0.0113	(0.6142, 0.9800, 0.1182)	Q1	Q1
P11	3	0.9409	−0.0113	(0.3901, 0.9409, 0.4263)	Q3	Q1
P11	4	0.9409	−0.0113	(0.5700, 1.2040, 0.3805)	Q1	Q1
P11	5	0.9409	−0.0113	(−0.5126, 0.9409, 0.0957)	Q4	Q2
P12	1	0.6377	0.0048	(−0.5700, 1.0656, 0.5215)	Q2	Q2
P12	2	0.6377	0.0048	(0.6408, 0.9800, 0.1025)	Q1	Q1
P12	3	0.6377	0.0048	(0.4110, 0.6377, 0.3804)	Q3	Q1
P12	4	0.6377	0.0048	(0.5700, 1.2110, 0.4807)	Q1	Q1
P12	5	0.6377	0.0048	(−0.6696, 0.6377, 0.1089)	Q4	Q2
P13	1	0.6309	−0.0292	(−0.5700, 1.0272, 0.5745)	Q2	Q2
P13	2	0.6309	−0.0292	(0.5864, 0.9429, 0.2000)	Q1	Q1
P13	3	0.6309	−0.0292	(0.4008, 0.6309, 0.5314)	Q3	Q1
P13	4	0.6309	−0.0292	(0.4746, 1.0276, 0.6200)	Q1	Q1
P13	5	0.6309	−0.0292	(−0.6341, 0.6309, 0.1445)	Q4	Q2
P14	1	0.6025	−0.0207	(−0.4472, 1.0059, 0.4075)	Q2	Q2
P14	2	0.6025	−0.0207	(0.7153, 0.9661, 0.2000)	Q1	Q1
P14	3	0.6025	−0.0207	(0.4014, 0.6025, 0.3891)	Q3	Q1
P14	4	0.6025	−0.0207	(0.5809, 1.1686, 0.3711)	Q1	Q1
P14	5	0.6025	−0.0207	(−0.4212, 0.6025, 0.0861)	Q4	Q2
H1	1	0.7201	−0.0284	(−0.5700, 1.0383, 0.3840)	Q2	Q2
H1	2	0.7201	−0.0284	(0.6049, 0.9622, 0.2000)	Q1	Q1
H1	3	0.7201	−0.0284	(0.4034, 0.7201, 0.3947)	Q3	Q1
H1	4	0.7201	−0.0284	(0.4991, 1.0809, 0.3781)	Q1	Q1
H1	5	0.7201	−0.0284	(−0.6233, 0.7201, 0.1105)	Q4	Q2
H2	1	0.7358	−0.0175	(−0.5700, 1.0559, 0.4661)	Q2	Q2
H2	2	0.7358	−0.0175	(0.7259, 0.9800, 0.1001)	Q1	Q1
H2	3	0.7358	−0.0175	(0.4679, 0.7358, 0.3742)	Q3	Q1
H2	4	0.7358	−0.0175	(0.5700, 1.2048, 0.4232)	Q1	Q1

Table 4 (continued)

ID	Block	H_{Limit}	$P_{\text{CurrentHMD}}\ (x)$	Automatic position NP_{VO}	$\phi(p)$	$\phi(NP_{\text{VO}})$
H2	5	0.7358	−0.0175	(−0.6354, 0.7358, 0.1068)	Q4	Q2
H3	1	0.6748	0.0146	(−0.4837, 1.0231, 0.5587)	Q2	Q2
H3	2	0.6748	0.0146	(0.5459, 0.9671, 0.2000)	Q1	Q1
H3	3	0.6748	0.0146	(0.3295, 0.6748, 0.3686)	Q3	Q1
H3	4	0.6748	0.0146	(0.5658, 1.1505, 0.5249)	Q1	Q1
H3	5	0.6748	0.0146	(−0.6076, 0.6748, 0.1152)	Q4	Q2
H4	1	0.6353	−0.0176	(−0.5700, 1.0326, 0.4262)	Q2	Q2
H4	2	0.6353	−0.0176	(0.7266, 0.9645, 0.2000)	Q1	Q1
H4	3	0.6353	−0.0176	(0.4291, 0.6353, 0.4099)	Q3	Q1
H4	4	0.6353	−0.0176	(0.5763, 1.1411, 0.4133)	Q1	Q1
H4	5	0.6353	−0.0176	(−0.6953, 0.6353, 0.1131)	Q4	Q2
H5	1	0.7425	−0.0050	(−0.5699, 1.0297, 0.4401)	Q2	Q2
H5	2	0.7425	−0.0050	(0.7207, 0.9712, 0.2000)	Q1	Q1
H5	3	0.7425	−0.0050	(0.4435, 0.7425, 0.3352)	Q3	Q1
H5	4	0.7425	−0.0050	(0.4590, 1.1393, 0.4156)	Q1	Q1
H5	5	0.7425	−0.0050	(−0.5817, 0.7425, 0.0961)	Q4	Q2
H6	1	0.7142	−0.0135	(−0.5700, 1.0165, 0.4485)	Q2	Q2
H6	2	0.7142	−0.0135	(0.5309, 0.9326, 0.2000)	Q1	Q1
H6	3	0.7142	−0.0135	(0.3745, 0.7142, 0.3994)	Q3	Q1
H6	4	0.7142	−0.0135	(0.4258, 1.0451, 0.4191)	Q1	Q1
H6	5	0.7142	−0.0135	(−0.6251, 0.7142, 0.1110)	Q4	Q2
H7	1	0.7201	0.0046	(−0.5700, 1.0383, 0.3840)	Q2	Q2
H7	2	0.7201	0.0046	(0.6049, 0.9622, 0.2000)	Q1	Q1
H7	3	0.7201	0.0046	(0.4034, 0.7201, 0.3947)	Q3	Q1
H7	4	0.7201	0.0046	(0.4991, 1.0809, 0.3781)	Q1	Q1
H7	5	0.7201	0.0046	(−0.6233, 0.7201, 0.1105)	Q4	Q2
H8	1	0.7852	0.0140	(−0.5700, 1.0316, 0.5137)	Q2	Q2
H8	2	0.7852	0.0140	(0.5783, 0.9676, 0.2000)	Q1	Q1
H8	3	0.7852	0.0140	(0.3942, 0.7852, 0.3432)	Q3	Q1
H8	4	0.7852	0.0140	(0.3990, 1.1072, 0.4955)	Q1	Q1
H8	5	0.7852	0.0140	(−0.5798, 0.7852, 0.0930)	Q4	Q2
H9	1	0.7420	−0.0210	(−0.5700, 1.0476, 0.4364)	Q2	Q2
H9	2	0.7420	−0.0210	(0.6338, 0.9800, 0.1115)	Q1	Q1
H9	3	0.7420	−0.0210	(0.3977, 0.7420, 0.3973)	Q3	Q1
H9	4	0.7420	−0.0210	(0.5700, 1.2164, 0.4327)	Q1	Q1
H9	5	0.7420	−0.0210	(−0.6428, 0.7420, 0.0999)	Q4	Q2
H10	1	0.7296	−0.0776	(−0.4333, 1.0629, 0.4140)	Q2	Q2
H10	2	0.7296	−0.0776	(0.6543, 0.9800, 0.0926)	Q1	Q1
H10	3	0.7296	−0.0776	(0.4140, 0.7296, 0.3411)	Q3	Q1
H10	4	0.7296	−0.0776	(0.5700, 1.2150, 0.3887)	Q1	Q1
H10	5	0.7296	−0.0776	(−0.7318, 0.7296, 0.1058)	Q4	Q2

Acknowledgements Grant PID2020-117361RB-C21 and PID2020-117361RB-C22 funded by MICIU/AEI/10.13039/501100011033.

Data availability The anonymized data generated during the experimentation sessions of this work is available through the Accessible-Rehab repository at https://github.com/AIR-Research-Group-UCLM/Accessible-Rehab. The repository also includes the source code related to the algorithms described in the article.

References

Anderson A, Alexanders J, Addington C, Astill S (2019) The effects of unimanual and bimanual massed practice on upper limb function in adults with cervical spinal cord injury: a systematic review. Physiotherapy 105(2):200–213. https://doi.org/10.1016/j.physio.2018.10.003

Blaga AD, Frutos-Pascual M, Creed C, Williams I (2024) VR-Grasp: a human grasp taxonomy for virtual reality. Int J Hum Comput Interact. https://doi.org/10.1080/10447318.2024.2351719

Brown JA (2006) Recovery of motor function after stroke. Prog Brain Res 157:223–228. https://doi.org/10.1016/S0079-6123(06)57015-3

Buckingham G (2021) Hand tracking for immersive virtual reality: opportunities and challenges. Front Virtual Real 2:728461

Chang L-R, Anand P, Varacallo M (2024) Anatomy, shoulder and upper limb, glenohumeral joint. In: StatPearls. StatPearls Publishing, Treasure Island (FL). http://www.ncbi.nlm.nih.gov/books/NBK537018/

Cheng Y, Wang Y (2022) Shared virtual reality experiences during the COVID-19 pandemic: exploring the gratifications and effects of engagement with immersive videos. Int J Environ Res Public Health. https://doi.org/10.3390/ijerph19095056

Chrysanthakopoulou A, Kalatzis K, Michalakis G, Michalellis I, Moustakas K (2022) ArtScape: gamified virtual reality art exploration. In: 2022 IEEE Conference on virtual reality and 3d user interfaces abstracts and workshops (VRW), pp 902–903. https://doi.org/10.1109/VRW55335.2022.00302. https://ieeexplore.ieee.org/abstract/document/9757469

Cluster of Health and Social Sciences, Singapore Institute of Technology, Singapore, Lo CN, Yeh T-T, Cluster of Health and Social Sciences, Singapore Institute of Technology, Singapore, Tan CT, Cluster of Infocomm Technology, Singapore Institute of Technology, Singapore, Tsang, EW, The Laboratory of Neuroscience for Education, Faculty of Education (2021) The University of Hong Kong, Hong Kong: a reliability and validity study on upper limb range of motion measurement using mobile sensor compared with goniometers. Iberoamerican J Med 3(3):227–233. https://doi.org/10.53986/ibjm.2021.0036

Dudley J, Yin L, Garaj V, Kristensson PO (2023) Inclusive Immersion: a review of efforts to improve accessibility in virtual reality, augmented reality and the metaverse. Virtual Real 27(4):2989–3020. https://doi.org/10.1007/s10055-023-00850-8

Finley M, Euiler E, Trojian T, Gracely E, Schmidt-Read M, Frye SK, Kallins M, Summers A, York H, Geigle PR (2020) Shoulder impairment and pain of individuals with newly acquired spinal cord injury compared to uninjured peers. Spin Cord Ser Cases 6:68. https://doi.org/10.1038/s41394-020-0318-1

Franz RL, Yu J, Wobbrock JO (2023) Comparing locomotion techniques in virtual reality for people with upper-body motor impairments. In: Proceedings of the 25th international ACM SIGACCESS conference on computers and accessibility. ASSETS '23. Association for Computing Machinery, New York, NY, USA, pp 1–15. https://doi.org/10.1145/3597638.3608394

Fujihara A, Ukimura O (2022) Virtual reality of three-dimensional surgical field for surgical planning and intraoperative management. World J Urol 40(3):687–696. https://doi.org/10.1007/s00345-021-03841-z

Golubović Š, Slavković S (2014) Manual ability and manual dexterity in children with cerebral palsy. Hippokratia 18(4):310

Herrera V, Vallejo D, Castro-Schez JJ, Monekosso DN, de Reyes A, Glez-Morcillo C, Albusac J (2023) Rehab-immersive: a framework to support the development of virtual reality applications in upper limb rehabilitation. SoftwareX 23:101412. https://doi.org/10.1016/j.softx.2023.101412

H. Hoppe A, Anken JK, Schwarz T, Stiefelhagen R, Van De Camp F (2020) CLEVR: a customizable interactive learning environment for users with low vision in virtual reality. In: Proceedings of the 22nd international ACM SIGACCESS conference on computers and accessibility. ASSETS '20: The 22nd International ACM SIGACCESS Conference on Computers and Accessibility. Virtual Event Greece Publisher: ACM, pp 1–4. https://doi.org/10.1145/3373625.3418009 (**ISBN: 9781450371032**)

Hutson J, Fulcher B (2023) A virtual reality educational game for the ethics of cultural heritage repatriation. Games Cult 18(6):759–782. https://doi.org/10.1177/15554120221131724

Javaid M, Haleem A (2020) Virtual reality applications toward medical field. Clin Epidemiol Glob Health 8(2):600–605. https://doi.org/10.1016/j.cegh.2019.12.010

Juan M-C, Elexpuru J, Dias P, Santos BS, Amorim P (2022) Immersive virtual reality for upper limb rehabilitation: comparing hand and controller interaction. Virtual Real. https://doi.org/10.1007/s10055-022-00722-7

Kalouaz A, Rooney B (2021) Virtual reality: towards universally accessible experiences

Kang HJ, Shin J-h, Ponto K (2020) A comparative analysis of 3D user interaction: how to move virtual objects in mixed reality. In: 2020 IEEE conference on virtual reality and 3d user interfaces (VR). IEEE, Atlanta, GA, USA, pp 275–284. https://doi.org/10.1109/VR46266.2020.00047. https://ieeexplore.ieee.org/document/9089474/

Kapandji A (2019) The physiology of the joints, vol. 1: the upper limb, 7th edn. Handspring, Singing Dragon, 123 S. Broad St., Ste 2750, Philadelphia, PA 19109. English, Paperback, p 368

Kim Y, Lee H (2022) Falling in love with virtual reality art: a new perspective on 3d immersive virtual reality for future sustaining art consumption. Int J Hum Comput Interact 38(4):371–382. https://doi.org/10.1080/10447318.2021.1944534

Lagos Rodriguez M, Garcia AG, Loureiro JP, Garcia TP (2022) Personalized virtual reality environments for intervention with people with disability. Electronics 11(10):1586. https://doi.org/10.3390/electronics11101586

Lee K-S, Zaman M, Hwang J (2022) Reduced muscle activity of the upper extremity in individuals with spinal cord injuries. Int J Environ Res Public Health 19(8):4708. https://doi.org/10.3390/ijerph19084708

Lim D, Hwang D, Cho KH, Moon C, Ahn SY (2020) A fully immersive virtual reality method for upper limb rehabilitation in spinal cord injury. Ann Rehabilit Med. https://doi.org/10.5535/arm.19181

Lin C-L, Chen S-J, Lin R (2020) Efficacy of virtual reality in painting art exhibitions appreciation. Appl Sci 10(9):3012. https://doi.org/10.3390/app10093012

Martin R, Silvestri J (2013) Current trends in the management of the upper limb in spinal cord injury. Curr Phys Med Rehabil Rep 1(3):178–186. https://doi.org/10.1007/s40141-013-0020-3

Martin JA, Ramsay J, Hughes C, Peters DM, Edwards MG (2015) Age and grip strength predict hand dexterity in adults. PLoS ONE 10(2):0117598. https://doi.org/10.1371/journal.pone.0117598

Mateo S, Roby-Brami A, Reilly KT, Rossetti Y, Collet C, Rode G (2015) Upper limb kinematics after cervical spinal cord injury: a review. J Neuroeng Rehabil 12(1):9. https://doi.org/10.1186/1743-0003-12-9

Mathiowetz V, Volland G, Kashman N, Weber K (1985) Adult norms for the box and block test of manual dexterity. Am J Occup Ther 39(6):386–391. https://doi.org/10.5014/ajot.39.6.386

Mc Kittrick A, Desselle MR, Padilha Lanari Bo A, Zhang B, Laracy S, Tornatore G (2023) Patient experience in adjunct controller-free hand tracking virtual reality tasks for upper-limb occupational therapy rehabilitation. J Patient Exp 10:23743735231211984. https://doi.org/10.1177/23743735231211983

McGrath J (2015) Hand dexterity in neuronal disorders: a range of abilities. PLoS ONE 10(2):0117598
Meta: hand tracking. https://www.meta.com/en-gb/help/quest/articles/headsets-and-accessories/controllers-and-hand-tracking/hand-tracking/ Accessed 12 Apr 2024
Mott M, Cutrell E, Gonzalez Franco M, Holz C, Ofek E, Stoakley R, Ringel Morris M (2019) Accessible by design: an opportunity for virtual reality. In: 2019 ieee international symposium on mixed and augmented reality adjunct (ISMAR-Adjunct), pp 451–454. https://doi.org/10.1109/ISMAR-Adjunct.2019.00122. https://ieeexplore.ieee.org/abstract/document/8951960
Othman A, Chemnad K, Hassanien A, Tlili A, Zhang C, Al-Thani D, Altinay F, Chalghoumi H, Al-Khalifa H, Obeid M, Jemni M, Al-Hadhrami T (2024) Accessible metaverse: a theoretical framework for accessibility and inclusion in the metaverse. Multimodal Technol Interact 8:21. https://doi.org/10.3390/mti8030021
Ambrosio AP, Fidalgo MI (2020) Past, present and future of virtual reality: analysis of its technological variables and definitions. Cult Hist Digit J. https://doi.org/10.3989/chdj.2020.010
Petrizzo I, Mikellidou K, Avraam S, Avraamides M, Arrighi R (2023) Reshaping the peripersonal space in virtual reality. https://doi.org/10.21203/rs.3.rs-3101264/v1
Phelan I, Furness PJ, Dunn HD, Carrion-Plaza A, Matsangidou M, Dimitri P, Lindley S (2021) Immersive virtual reality in children with upper limb injuries: findings from a feasibility study. J Pediatr Rehabilit Med 14(3):401–414. https://doi.org/10.3233/PRM-190635
Pietroszek K (2018) Raycasting in virtual reality. In: Lee N (ed) Encyclopedia of computer graphics and games. Springer, Cham, pp 1–3. https://doi.org/10.1007/978-3-319-08234-9_180-1
Postolache O, Hemanth DJ, Alexandre R, Gupta D, Geman O, Khanna A (2021) Remote monitoring of physical rehabilitation of stroke patients using IoT and virtual reality. IEEE J Sel Areas Commun 39(2):562–573. https://doi.org/10.1109/JSAC.2020.3020600
RajKumar A, Vulpi F, Bethi SR, Wazir HK, Raghavan P, Kapila V (2020) Wearable inertial sensors for range of motion assessment. IEEE Sens J 20(7):3777–3787. https://doi.org/10.1109/JSEN.2019.2960320
Soliman M, Pesyridis A, Dalaymani-Zad D, Gronfula M, Kourmpetis M (2021) The application of virtual reality in engineering education. Appl Sci 11(6):2879. https://doi.org/10.3390/app11062879
Soomal HK, Poyade M, Rea PM, Paul L (2020) Enabling more accessible MS rehabilitation training using virtual reality. Adv Exp Med Biol 1262:95–114. https://doi.org/10.1007/978-3-030-43961-3_5
Tokgöz P, Wähnert D, Elsner A, Schack T, Cienfuegos Tellez MA, Conrad J, Vordemvenne T, Dockweiler C (2023) Virtual reality for upper extremity rehabilitation-a prospective pilot study. Healthcare 11(10):1498. https://doi.org/10.3390/healthcare11101498
Using apple vision pro for advanced interaction. Accessed 15 Apr 2023. https://support.apple.com/en-us/117741
Valente L, Feijó B, Ribeiro A, Clua E (2016) The concept of pervasive virtuality and its application in digital entertainment systems. In: Wallner G, Kriglstein S, Hlavacs H, Malaka R, Lugmayr A, Yang H-S (eds) Entertainment computing—ICEC 2016. Springer, Cham, pp 187–198. https://doi.org/10.1007/978-3-319-46100-7_16
Venkatesan M, Mohan H, Ryan JR, Schürch CM, Nolan GP, Frakes DH, Coskun AF (2021) Virtual and augmented reality for biomedical applications. Cell Rep Med 2(7):100348. https://doi.org/10.1016/j.xcrm.2021.100348
Vlahovic S, Suznjevic M, Skorin-Kapov L (2022) A framework for the classification and evaluation of game mechanics for virtual reality games. Electronics 11(18):2946. https://doi.org/10.3390/electronics11182946
Wang X, Fu Y, Ye B, Babineau J, Ding Y, Mihailidis A (2022) Technology-based compensation assessment and detection of upper extremity activities of stroke survivors: systematic review. J Med Internet Res 24(6):34307. https://doi.org/10.2196/34307
Wazir HK, Gaikwad K, Kapila V (2022) Range of motion assessment using a digital voice assistant. In: 2022 44th annual international conference of the IEEE engineering in medicine & biology society (EMBC), pp 2577–2580. https://doi.org/10.1109/EMBC48229.2022.9870888. (**ISSN: 2694-0604**)
Xiao B, Chen L, Zhang X, Li Z, Liu X, Wu X, Hou W (2022) Design of a virtual reality rehabilitation system for upper limbs that inhibits compensatory movement. Med Nov Technol Devices 13:100110. https://doi.org/10.1016/j.medntd.2021.100110
Ying T, Tang J, Ye S, Tan X, Wei W (2022) Virtual reality in destination marketing: telepresence, social presence, and tourists' visit intentions. J Travel Res 61(8):1738–1756. https://doi.org/10.1177/00472875211047273